EXPERIMENTAL DETERMINATION OF EFFECTIVE BREADTH OF WIDE FLANGE SECTIONS

John Francis Hamma

EXPERIMENTAL DETERMINATION OF EFFECTIVE BREADTH OF WIDE FLANGE SECTIONS

by

John Francis Hamma, LT, USN

B.S., University of Michigan
(1963)

Submitted in partial fulfillment
of the requirements for the
Degrees of

Naval Engineer

and

Master of Science
(Mechanical Engineering)

at the

Massachusetts Institute of Technology

June, 1970

ABSTRACT

Experimental Determination of Effective Breadth of Wide Flange Sections.

John Francis Hamma, LT, USN.

Submitted to the Department of Naval Architecture and Marine Engineering and the Department of Mechanical Engineering on 21 May 1970 in partial fulfillment of the requirement for the degrees of Naval Engineer and Master of Science (Mechanical Engineering).

In a structure containing plating and stiffeners, any given portion containing an expanse of plating and one stiffener can be thought of as a wide-flanged beam. Under axial or bending loads, the distribution of longitudinal stress across the flange is such that the maximum stress occurs above the web and tapers off to a finite value at the edge of the flange. For computational purposes, it would be more convenient to consider a constant stress level in the flange. The "effective breadth" of the flange (plating) is defined as that portion of the flange which, if uniformly stressed, would carry the same load as carried by the actual flange.

Tests were run on a T-section in axial compression and in a bending mode with compression in the flange, and on a box girder in the bending mode. The results of the tests on the T-section are in close agreement with the theory. The box girder tests yielded results that are thought to be inapplicable to the theory because of failure to maintain the external conditions to which the theory applies.

Thesis supervisor: Alaa E. Mansour
Title: Assistant Professor of Naval Architecture

TABLE OF CONTENTS

NOMENCLATURE

B	Breadth of the beam
b	1/2 breadth of the beam
cL	Length between points of zero moment
E	Young's modulus
e	Strain
I	Moment of inertia
L	Length of the beam
M	Moment
N.A.	Neutral axis
x, 1	Direction along the web of the beam
y, 2	Direction perpendicular to the web of the beam
$\bar{y}$	Location of the neutral axis of a member from the top flange
Z_{fl}	Section modulus at the flange
Z_w	Section modulus at the toe of the web
λ	1/2 effective breadth of the beam
λ/b	Effective breadth ratio
σ	Stress
μ	Poisson's ratio
φ	Angular direction of the larger principal stress with respect to a given axis

INTRODUCTION

A large portion of a ship's structure is comprised of a combination of flat plate and stiffeners. Any given portion of such a structure containing an expanse of plating and one stiffener can be thought of as a beam with an exceptionally wide flange. It is often convenient to do just that for purposes of computation, permitting the use of beam theory on various parts of the ship's structure.

Whereas simple beam theory assumes that the stress at any given distance from the neutral axis is uniform in a plane parallel to the neutral axis at that distance, this is not the case when considering the above mentioned structure as a wide flange beam. In particular, when the plating is loaded primarily by transmission of a shear force through the webs of the stiffeners, the magnitude of the stress in the plating decreases with increasing distance from the web. The "effective breadth" of the flange (plating) is defined as that portion of the flange which, if uniformly stressed, would carry the same load as carried by the actual flange. This is illustrated in figure 1.

The effective breadth of a plate is dependent upon loading conditions, section geometry (including length-to-breadth ratio) and boundary conditions.

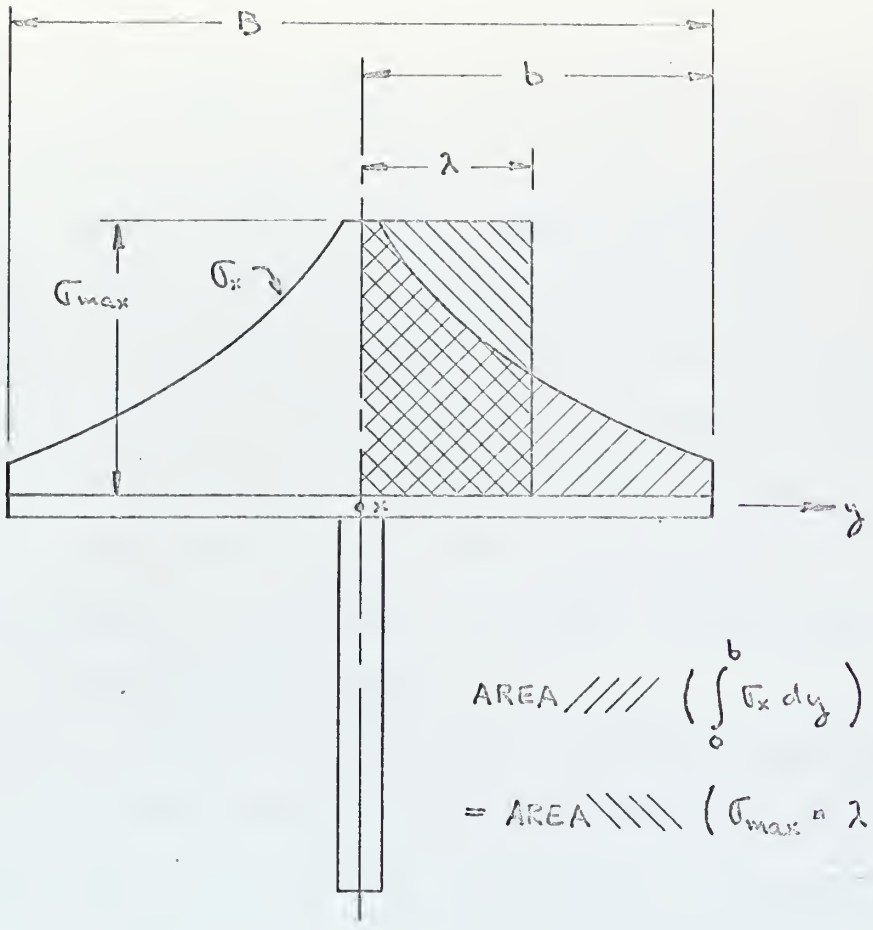

σ_{max} = MAXIMUM STRESS IN SECTION.

σ_x = STRESS IN DIRECTION PARALLEL TO WEB.

λ = 1/2 EFFECTIVE BREADTH OF SECTION.

b = 1/2 FULL BREADTH OF SECTION.

λ/b = RATIO OF EFFECTIVE BREADTH TO FULL BREADTH, OR EFFECTIVENESS RATIO.

FIGURE 1. EXPLANATION OF EFFECTIVE BREADTH.

Curves of effective breadth ratios (λ/b) have been plotted in reference (1) as a function of the length to breadth ratio (cL/B) of the member, where "cL" is the length between points of zero bending moment, and in reference (3) as a function of L/B, where L implies the load carrying portion of the member only. Loading conditions and section geometry are treated as independent parameters. In all the curves, (λ/b) approaches 1.0 with increasing L/B, as the beam approaches normal beam proportions and beam theory applies.

Schade has analyzed the effective breadth of stiffened plating in bending for several loading conditions: uniformly distributed, sinusoidally distributed, triangularly distributed, and concentrated; structural configurations of single, double and multiple webs were investigated (1).* He later extended his analysis to include unsymmetrical stiffener arrangements and variations on the loading patterns (2). Mansour (3) considered the effective breadth concept for the loading conditions of a constant axial load and a uniform bending moment.

The experiments undertaken in this thesis relate primarily to Mansour's work. Two beam configurations--

* Numbers in parentheses designate particular references.

T-section and box girder--were tested in bending and axial compression. The bending loads were applied such as to give a uniform moment distribution over the major portion of the beam. The principal stresses were measured across the mid-span of the beam, and the effective breadth compared with that predicted by theory.

PROCEDURE

The test specimens were supported and loaded in the test frame built for this purpose, and described in appendix A. Both specimens were simply supported for all test runs. Load was supplied by a hydraulic jack system.

Tests were run on the T-section in axial compression and in bending with compression in the flange. The box girder was tested in the bending condition only.

A quick stress analysis was made prior to loading to determine the maximum permissible pump pressure in order not to yield any portion of the sample. It was not necessary for the purposes of these tests to put high stress levels on the flanges of the beam. The stress pattern would theoretically remain the same up to the yield point. Tests at different magnitudes of the same loadings were run to confirm this, and to add a confidence factor to the data.

Two sets of readings were taken and averaged at zero load and at each successive load, to attempt to compensate for random fluctuations in the output of the digital strain indicator. The principal stresses were determined from the average strain readings. The principal stress in the longitudinal direction was plotted non-dimensionally as a

fraction of the longitudinal stress directly above the web in the case of the T-section. Actual stresses were plotted for the box girder. The effective breadth of the sample for each load was found by taking the area under the curve with a planimeter. This area, divided by the maximum compressive stress (for cases where compression is expected) times the breadth of the flange, is the effective breadth ratio (λ/b), also called "effective breadth" and "effectiveness."

RESULTS

The following pages show the results of the test runs. Test runs were numbered consecutively from one. However, for various reasons explained in Appendix B, the results of some were incomplete or inconclusive.

This section consists of a summary of expected results and experimental results, followed by the curves of stress distribution of the principal stress across the width of the flange, for each beam specimen and each loading condition. The test runs covered are: axial compressive load on T-section, bending load on T-section, and bending load on the box girder.

Results of test runs 3 and 4, axial compression.

L/B = 28/18 = 1.56

From Mansour's theory, reference 3, expected $\lambda/b = .63$.

Effective area at $\lambda/b = .63$: 5.58 in^2 (from figure B3).

	Run 3	Run 4
Jack pressure	4200 psi	7025 psi
Ram area	5.1572 in^2	5.1572 in^2
Force, F	21,600 lbs	36,220 lb
σ_{max} expected	-3890 psi	-6500 psi
σ_{max} actual	-4840 psi	-8250 psi
λ/b actual	.592	.557

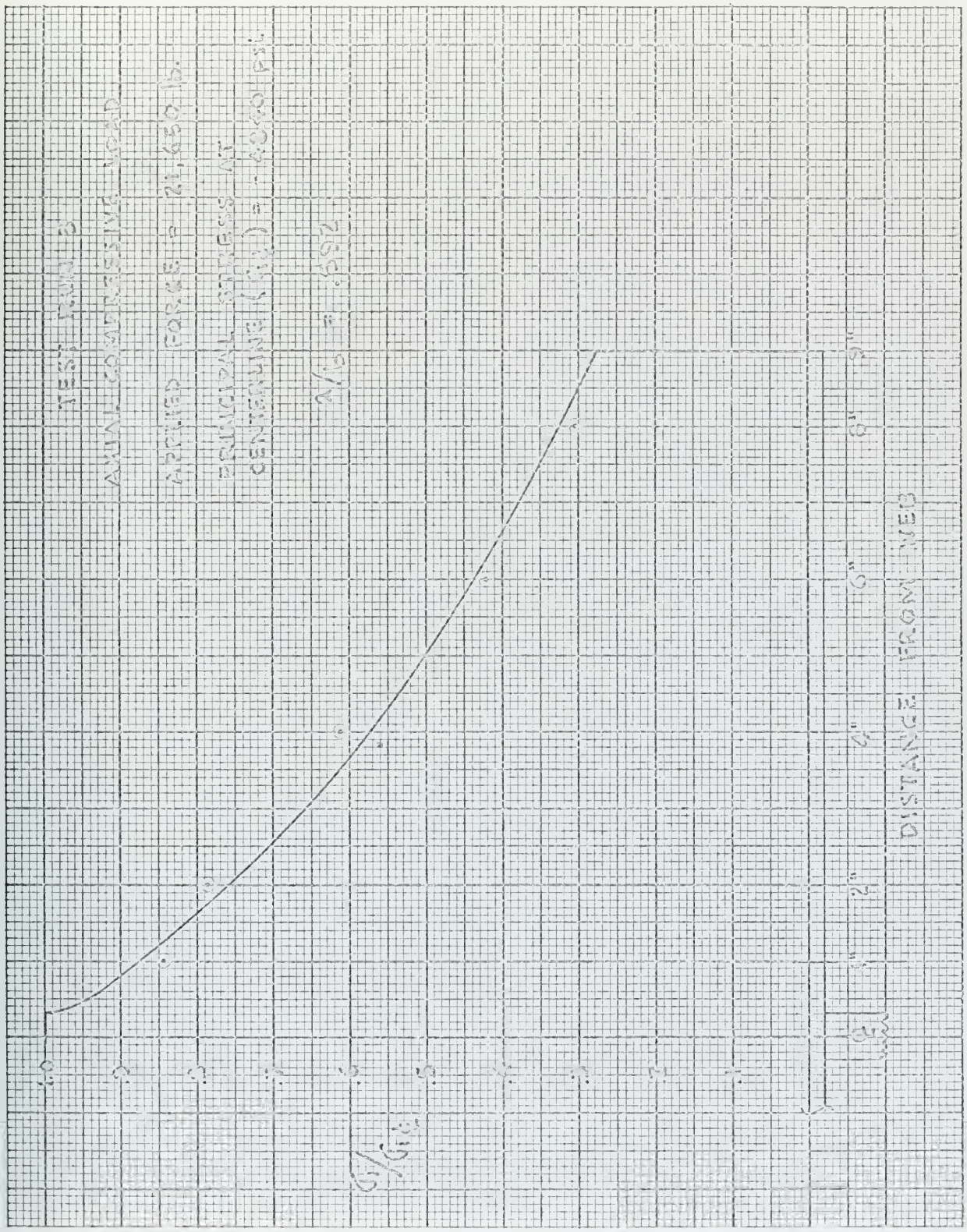

Figure 2. Results of test run 3.

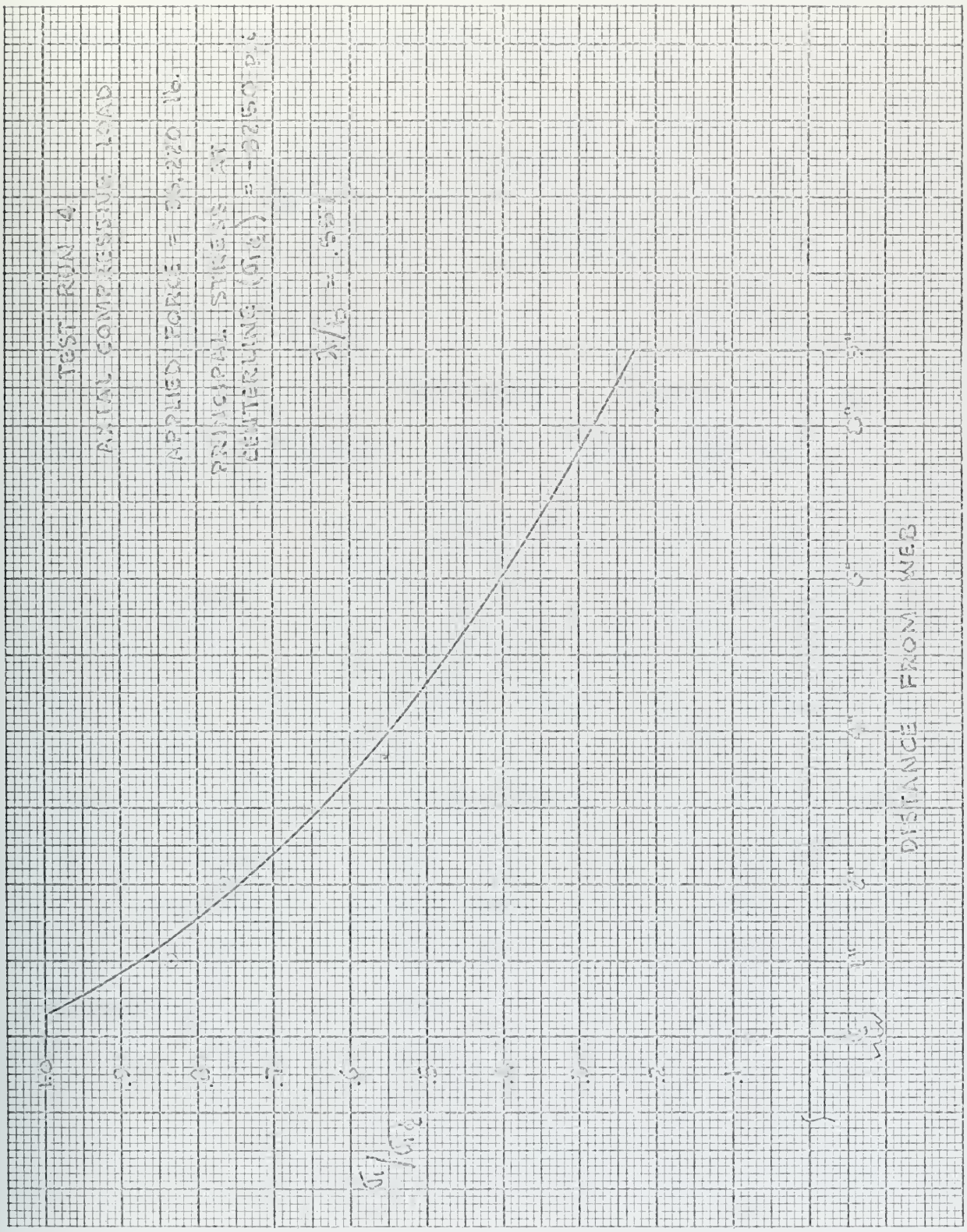

Figure 3. Results of test run 4.

Results of test runs 6 and 7, bending.

cL/B = 26/18 = 1.445

From Mansour's theory, reference 3, expected λ/b = .60.

Effective section modulus at λ/b = .60: 9.50 in^3
(from figure B3).

	Run 6	Run 7
Jack pressure	2300 psi	4500 psi
Ram area	5.1572 in^2	5.1572 in^2
Force, F	11,850 lb	23,150 lb
Lever arm, l	4"	4"
Applied moment	-47,400 in-lb	-92,600 in-lb
Section modulus	9.50 in^3	9.50 in^3
σ_{max} expected	-4980 psi	-9750 psi
σ_{max} actual	-4700 psi	-9410 psi
λ/b actual	.581	.581

Figure 4. Results of test run 6.

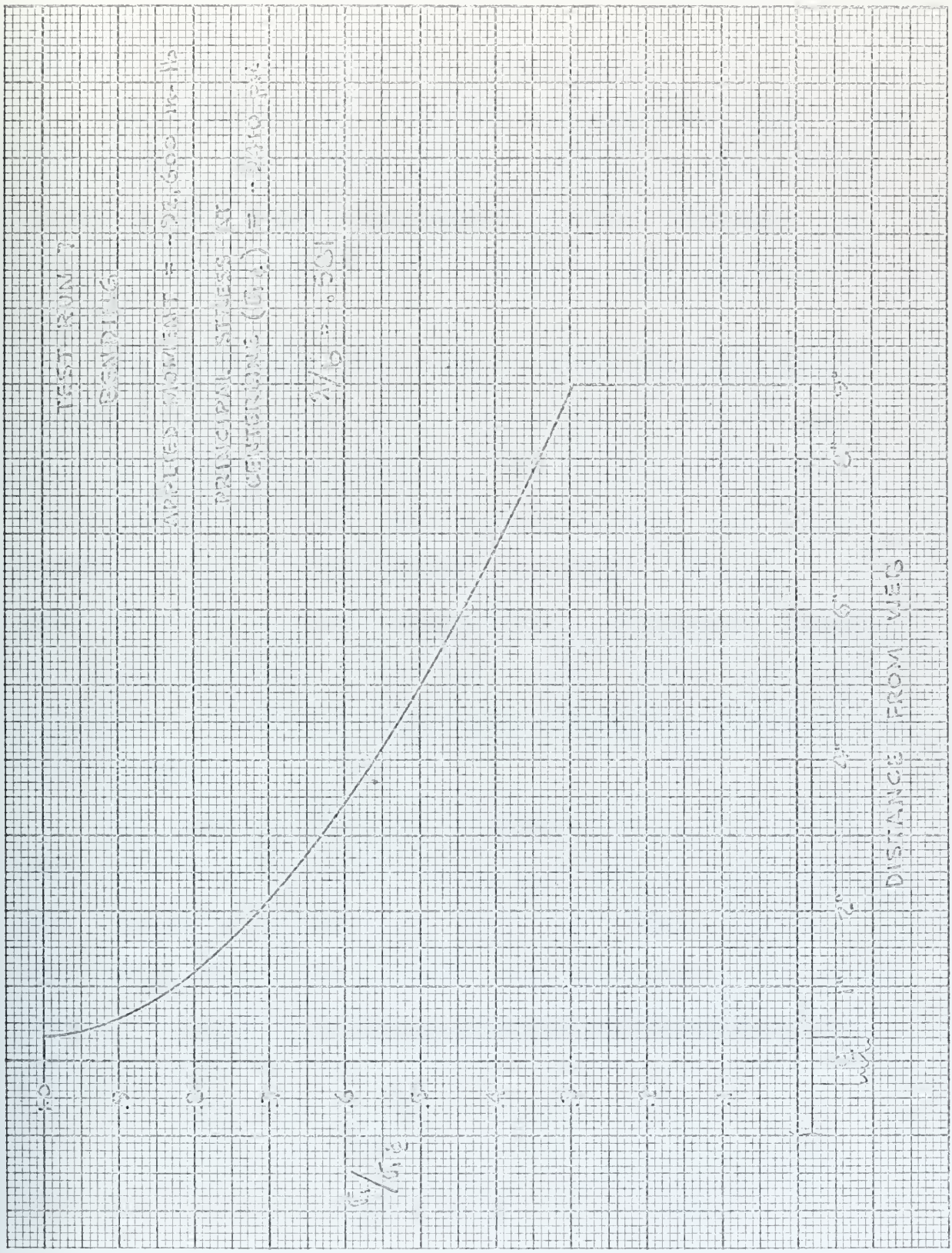

Figure 5. Results of test run 7.

RESULTS OF BOX GIRDER TESTS, BENDING LOAD

Approximately 15 different test runs were made on the box girder. The results of 6 of them are shown in figure 6 and 7. The results are not at all what was expected; a discussion of the results appears in the following section.

The girder was loaded first on the webs, as shown schematically in figure A6. Lever arms of 4", 7" and 12½" were used, and moments in the vicinity of 30,000 in-lb and 58,000 in-lb were applied in each case. The girder was then loaded through the flange, with an additional bar of 12¼" length bearing between the loading bar shown in figure A6 and the flange. These loads were applied at 4" and 12½" lever arms at moments in the 30,000 in-lb range.

The expected λ/b from reference 3 was .86. At this effective breadth ratio, the maximum stress experienced in the flanges at 30,000 in-lb should have been -7900 psi. The actual values are shown in figures 6 and 7. At 58,000 in-lb, the maximum stresses experienced should have been -15,300 psi.

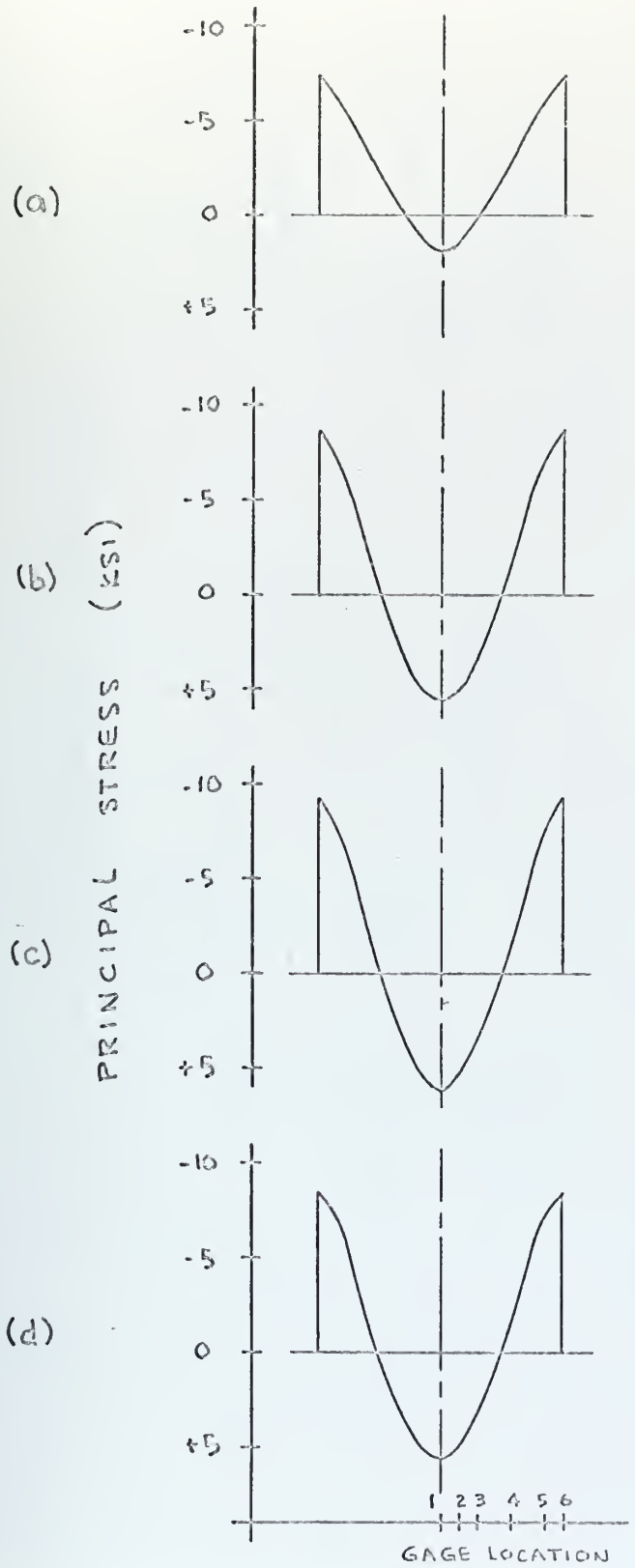

Run 8. Initial loading.
4" lever arm. Load
applied to webs.
Moment = 29,950 in-lb.
σ max ≈ -7500 psi.
λ/b = .314

Run 13. Bending load.
4" lever arm. Load
applied to webs.
Moment = 31,400 in-lb.
σ max ≈ -8700 psi.
λ/b = .085

Run 11. Bending load.
7" lever arm. Load
applied to webs.
Moment = 30,700 in-lb.
σ max ≈ -9200 psi.
λ/b = .075

Run 14. Bending load.
12 1/2" lever arm. Load
applied to webs.
Moment = 32,900 in-lb.
σ max ≈ -8450 psi.
λ/b = .094

Horizontal scale:
1 box = 1"

FIGURE 6. RESULTS OF BOX GIRDER TESTS.

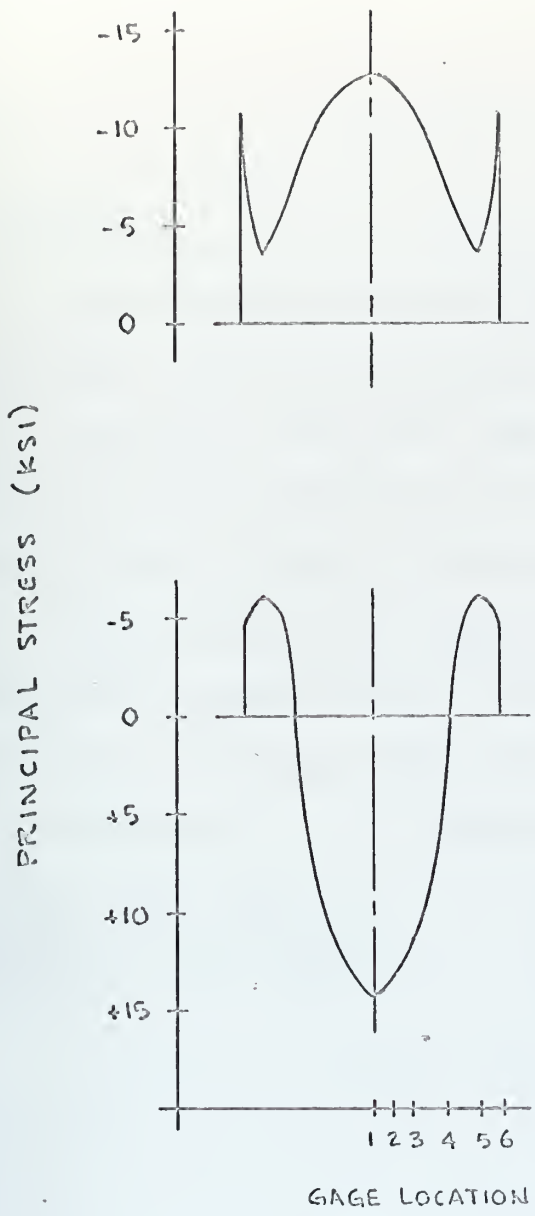

Run 15. Bending load applied to the flange at a lever arm of $12\frac{1}{2}$". Moment = 32,200 in-lb.

Run 16. Bending load applied to the flange at a lever arm of 4". Moment = 27,300 in-lb.

Horizontal scale:
1 box = 1 inch

Figure 7. Results of box girder tests.

DISCUSSION OF RESULTS

T-SECTION

The results of the tests are qualitatively what was expected. That is, the maximum stress occurs at the web, and tapers off toward the edge. The numerical results are thought to be satisfactory, but there are aspects of each result that are open to discussion.

In each case, the experimentally found values of the effective breadth ratio, λ/b, are lower than those predicted by theory. The specific values are:

loading	theoretical	experimental	error
axial, light (run 3)	.63	.592	6.0 %
axial, heavy (run 4)	.63	.557	11.6 %
bending, light (run 6)	.60	.581	3.2 %
bending, heavy (run 7)	.60	.581	3.2 %

It might be expected that the experimental values would be lower than theoretical values, as ideal conditions are never achieved in the laboratory. This will be discussed in the general comments at the end of this section.

It is interesting to note that the experimentally determined value of λ/b decreased with the increased load on the axial compression tests. It remained the same for both loads on the bending tests. The only external that occurred in going from light load to heavy load in each type of test

was the increase in oil pressure in the cylinders. That is, the load was not removed between tests, and so there was no possibility that there would be any difference in the applied loads, except for the magnitude. In view of this, it is concluded that some buckling of the flange occurred in the heavily loaded axial test that did not occur in the lightly loaded test. It is possible that there was some buckling in each test; this cannot be determined from these two experiments.

It is noted that the maximum stress expected from theory is less than the maximum stress obtained during the experiments. One would expect to find this trend, since a greater effective breadth is predicted by the theory than was found in the experiment. It is noted, however, that percentage increase in the stress is larger than the percentage decrease in the effective breadth. For example, in run 3 the theoretically predicted maximum stress was -3890 psi; the maximum experimental stress was -4840 psi, or an increase of 24.4% over the predicted value. However, the experimentally determined λ/b of .592 was only 6.0% lower than the theoretical value of .63. The reason why the percentage increase in stress is not equal to the percentage decrease in the effective breadth ratio is not immediately apparent.

Rosettes were used to measure the strain in order to ascertain that the principal stresses were parallel and perpendicular to the web. This was strongly suspected to be the case initially, and the small angles obtained in the calculations shown in Appendix B confirm this.

BOX GIRDER

The results of the box girder tests were quite different from those expected. It would be anticipated that this girder, loaded on the webs and with a uniform bending moment over the center of its span, would yield a stress distribution at midspan as shown in figure (a).

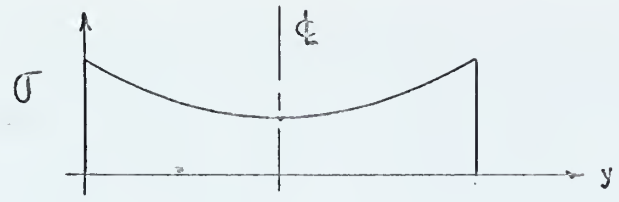

(a)

A compressive stress is expected with the loading used in these experiments.

The results of the 4 test runs shown in figure 6 exhibit the same qualitative shape, but the numerical values of the stress vary greatly from those expected. The effective breadth ratio of this beam is theoretically .86 (figure B2). With the exception of the very first test run on the beam, the experimental values of λ/b are in the vicinity of

.10 and lower. The value found on the initial run is .314.

The combination of the extremely low λ/b values, and the drop between the value found in the initial run and those subsequent to it, led the author to believe that some mechanism such as local buckling, membrane effects in the flanges, non-uniform shear transmission into the flange, or a combination of these, is acting on the flange in addition to the expected shear lag effect.

The critical stress for local buckling of a perfectly straight plate can be determined by the formula

$$\sigma_{cr} = \frac{k \pi^2 E}{12(1-\mu^2)} \left(\frac{t}{B}\right)^2$$

where k is a coefficient representing various end conditions and aspect ratios, E, μ, t and B are as previously defined. Timoshenko (5) gives a k value of approximately 2.2 for long plates in a condition of simple support on 2 edges and unsupported on the loaded edges. With the flanges intermittantly welded to the webs of this girder, it is anticipated that the end conditions would lie between simply supported and fixed, closer to simply supported. The corresponding value of critical stress is 5060 psi. Any initial distorsion in the plate would change this value slightly.

It seems likely that test run 9, which was an extension

of run 8 with a heavier load applied, caused local buckling and high membrane stresses in the flanges. Data for this run, presented in appendix C, shows that the principal stress experienced by the flange was approximately -11,000 psi. It is highly probable, therefore, that local buckling occurred on the second test run made on this specimen. Succeding runs were then subject to whatever permanent deformation may have been incurred during this buckling. Permanent deformation is indicated by the "zero" readings taken after the release of the load.

The reverse in curvature of the principal stress plots toward the webs (see figure 6) was inferred from the readings of gage number 10 on test runs 13 on. This gage was added to the specimen to give information about the stresses at the edge of the flange where the weldments prevented the installation of strain gages. This assumes that the stress is transmitted unchanged from the web to the flange, which is not strictly true, as discussed later.

However, the reverse curvature toward the flange is characteristic of post-buckling behavior when membrane stresses develop. Work in this area has been done by Mansour, reference 6.

The non-linearity of the measured strains with the increasing load, as evidenced in runs 8, 9 and 10, and runs

11 and 12, is further indication of buckling.

A comparison of internal and external moments (numerical work in appendix B), shows that the internal moments, as determined from the strain gage readings, are considerably lower than the applied moment. One possible explanation of this is given by Schade (7). He tested a box girder 42' x 8' x 4'-8", under loads such as to give a saddle-shaped bending moment (figure b).

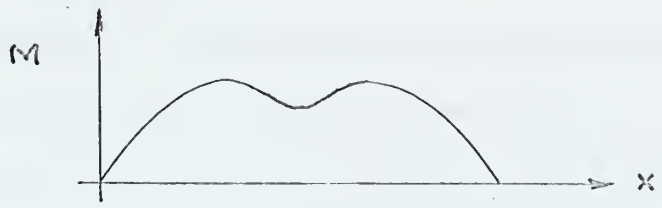

(b)

The results of the tests with this applied moment showed that maximum longitudinal stress occurred at the centerline, and not only attenuated, but actually reversed sign toward the webs. The expected results before the tests had been similar to those expected in this thesis and previously sketched in figure (a). Schade concluded that this expected stress distribution is a special case, and that the stress distribution in general is dependent on the shape of the applied moment curve. It must be noted that the curves determined from Schade's tests do not exhibit the reverse curvature toward the webs that these results exhibit.

The applied moments should give an external bending moment curve as shown in figure (c).

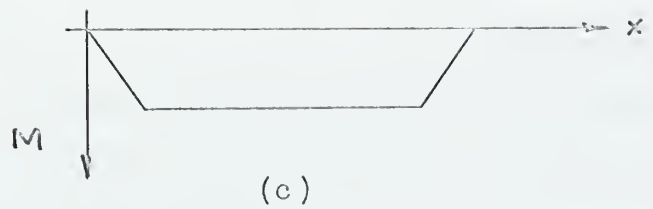

(c)

Perhaps the lower load carried by the flange in these tests is due to the intermittant fillet welds causing an uneven distribution of forces in the flange by the non-continuous transmission of shear force from web to flange. The average length of weld and spacing was $1\frac{1}{2}$" and 2" respectively. This was not uniform over the length of the specimen, but close to it. The location of the load application with respect to a weld or a space varied for different test runs, and in fact varied from one end of the specimen to the other. It is possible that this had some unknown effect on the distribution of the load over the length of the flange.

The results presented in figure 6 -- loading through the webs -- seem to have been influenced by a combination of the 3 mechanisms discussed. That is, local buckling, non-uniform shear transmission to the flange, and shear lag effects are all interacting in some manner.

For runs 15 and 16, the test specimen was loaded

through the flanges. As had been initially suspected, local effects of the loading prevailed, and the results are indicative of plate membrane and bending action rather than beam bending. During these tests, some distorsion occurred to the flange directly below the loading bar and to the tips of the webs adjacent to it. Results and data are included for information.

GENERAL COMMENTS ON THE RESULTS AND PROCEDURES.

It was mentioned previously that less than ideal results were to be expected in the laboratory. Some of the conditions which it is felt contributed to this are discussed.

The theory presented by Mansour in reference 3 is applicable to beams under axial tensile load or uniform bending moment. The application of such loads with no side effects is difficult at best. The axial load used in these experiments was applied by centering the plunger surface of the cylinder about the neutral axis at each end of the beam and exerting force. A slight misalignment of the cylinders would induce unwanted bending moments into the beam.

The same potential for error is involved in the bending tests. It was desired to place the load directly over the

web and in perfect alignment with the direction of the web. The small angles of principal stresses from the longitudinal obtained in test runs 6 and 7 indicate that the loading was quite good. However, previous runs 1, 2 and 5, under the theoretically same loading condition, indicated that principal stresses ran at angles of 5 to 10 to the longitudinal. In fact, runs 1 and 2 indicated that the angle of offset from the longitudinal was in the opposite direction from that indicated by run 5. That is to say, one run produced results indicated in sketch (d) while the other run produced that indicated in (e): (angles exaggerated)

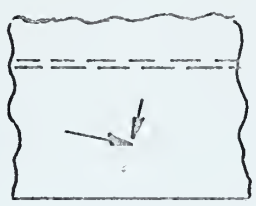

(d)

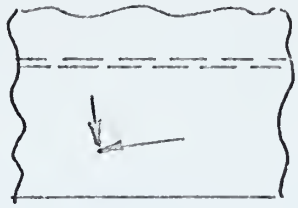

(e)

The calculations are not included in this report, but the original data appears in appendix C. The relative sizes of the strains in the shear arms of the strain gages in runs 1 and 2, compared with those in run 5, indicate this effect. Since this reversal of direction occurred, and since an attempt to apply the load in runs 6 and 7 more carefully seemed to reduce the angle involved, it was concluded that the bending sample was very sensitive to the

external loading, and that misalignment of this load was responsible for the principal stresses being skewed to the longitudinal and transverse directions.

The importance of the careful selection and application of the strain gages was clearly demonstrated during these experiments. An initial attempt was made to use some old wire gages that were on hand. Their age and the history of their storage were unknown, although the packages were still sealed and they appeared to be in excellent condition before installation on the test specimen. However, after installation, it was impossible to zero several of them on the digital strain indicator, and some of them gave erratic results during tests. Time and effort was wasted in trying to economize in this area.

Two sets of strain readings were taken at each zero stress level and each loading, and the average used in the stress calculations. Generally, the agreement of the two readings was excellent, but as in all experimental work, some scatter must be expected. A difference of 3 or 4 percent in these readings was considered to be acceptible.

The test specimens themselves were not perfect. The welding of the relatively thick web of the T-section to the flange plate caused the flange to warp slightly around the web. Figure (f) shows an exaggerated picture of this.

(f)

The effects of this on the results are thought to be small, but are open to discussion.

Thin plating was specified for the box girder in hopes of keeping the required loading low, and to keep the weight low enough for convenient handling. The thin plating in turn raised fears of welding distorsion and the use of intermittant welds. As previously discussed, it is thought that this contributed to the unusual results obtained.

The material properties of the steel -- Young's modulus and Poisson's ratio -- are also subject to slight variation. However, it is felt that in comparison to the other factors affecting the results, this is negligible.

CONCLUSIONS

The results of the T-section tests are thought to be an accurate reflection of the objectives of this thesis. The desired external conditions were maintained throughout the tests. The results are in good agreement with the theory presented by Mansour in reference 3. These tests show that the effective breadth of the flange can be considerably less than the actual breadth, and that this should definitely be taken into account in the design of structures using wide flange beams, or built-up members acting as such.

Although the results of the box girder were not as expected for reasons that violated the conditions of the theory, the tests did in fact indicate that there can be a wide fluctuation in the stresses across the flanges of the girder. These tests were also useful in demonstrating the care that must be taken in properly anticipating the loading of various components of a structure.

RECOMMENDATIONS

It is recommended that additional tests be carried out on wide flange beams, both to further verify the results of the theory and to measure the effects of parameters not specifically covered by the theory. An example of the latter is the application of combined loads to the beams. It was desired to do this during this series of tests, but time and other factors prevented it.

More specific recommendations would include the exercise of a greater care in preparing the test specimens. It was noted that some welding distorsion took place on the T-section. Perhaps greater care in welding, or post-welding heat treatment, could prevent this. It would have been desirable to have had the box girder continuously welded, but again, the possibility of distorsion prevented it. One remedy for this would be the use of heavier plating; this would also increase the critical buckling load for the girder.

The use of more than 10 strain gages simultaneously presented inconveniences in the switching circuits. It is wise to have an arrangement that permits the operator to read all gages without leaving his seat to switch gages or to switch leads to the various electronic components. Doing

so introduces room for error in data recording.

It is also recommended that the greatest amount of care be taken in loading and supporting the test specimens. It is essential to reduce the number of unwanted side effects, as each of these presents a potential unknown effect on the results.

Aside from the first recommendation that the testing be continued, perhaps the most emphasis should be placed on the prior study of the problem. Detailed and exhaustive calculations should be performed to ensure that an unexpected condition, such as the local buckling of the box girder, will not prevent the tests from yielding useful results.

APPENDIX A- DESCRIPTION OF APPARATUS AND DETAILS OF PROCEDURE

Part of the time spent on this thesis involved the preparation of the Ship Structures Lab for use, and the design and construction of a test frame. The laboratory room had been in disuse for several years and had become a general storage area. There were the remains of several old thesis projects and various lab supplies which later proved useful. However, much of the equipment and tools normally found in a lab had to be bought or borrowed. The entire job of readying the lab for use took considerable time and effort.

It was desired to keep the test frame as simple as possible, yet provide enough flexibility as possible for use with different samples and different projects. A second, and very important, consideration was keeping costs to a minimum.

The resulting frame is shown in figure A1. The vertical members are 18" x 11 3/4" x 105# wide flange beams with flat bar stiffeners between the flanges, 5 feet long. These pieces existed as such from a past project. The horizontal members are new 8" x 8" x 31# wide flange beams,

FIGURE A1. TEST FRAME.

59" long. The beams are connected with a continuous fillet weld. Lateral support is provided by a 5 foot length of 1" by 12" steel plate, welded to the vertical members; these pieces were also existing among the old material in the lab.

The space between the horizontal members is 27". This was a compromise between a desire for the largest possible opening, to accomodate a variety of test specimens, and the desire to keep it small, to minimize the support and loading apparatus for the samples to be immediately studied. Twenty-seven inches was determined from the combination of what is thought to be a reasonable support structure, the height of the larger specimen, and required clearance for any of several size hydraulic jacks that were on hand or being considered for purchase.

The new horizontal members would have been chosen on one of two criteria: the lightest beam with an 8" flange, which was deemed to be the minimum width desirable for a support or hydraulic cylinder bearing surface; or the lightest beam that would be capable of taking full load of 2 hydraulic cylinders (20 tons each) spaced 6" to either side of the mid-span without excessive deflection. The former criterion controlled and the 8" x 8" x 31# wide flange was selected. The moment of inertia of this section

is 109.7 in^4. Considering the horizontal members to have built-in end conditions, the maximum stress experienced under the above mentioned load is 14.1 K.S.I. The deflection in this case would be .014". The deflections experienced with the maximum actual loadings would be less than half that.

The side beams have a moment of inertia of about 1800 in^4. The external loads placed on these beams were in the order of 18 tons, near the center of the frame. For all practical purposes, there was no deflection in these beams.

Hydraulic cylinders were used to apply the loads to the samples. Twenty ton capacity cylinders were readily available and had the working range necessary for all anticipated tests. Cylinder data follows:

Manufacturer: Blackhawk Mfg. Co., Milwaukee, Wis.
Model: RC 251
Capacity: 20 tons
Plunger travel: 5"
Plunger diameter: 2¼"
Oil Capacity: 26 cubic inches
Effective ram area: 5.1572 square inches
Weight: 22 3/4 pounds

The base of the cylinder bore directly on the test frame members, and in the majority of cases, the plunger head bore directly on the test specimen. The plunger bearing surface was a 2¼" diameter section. For 2 test runs, a smaller bearing plug of 3/4" diameter rod was attached

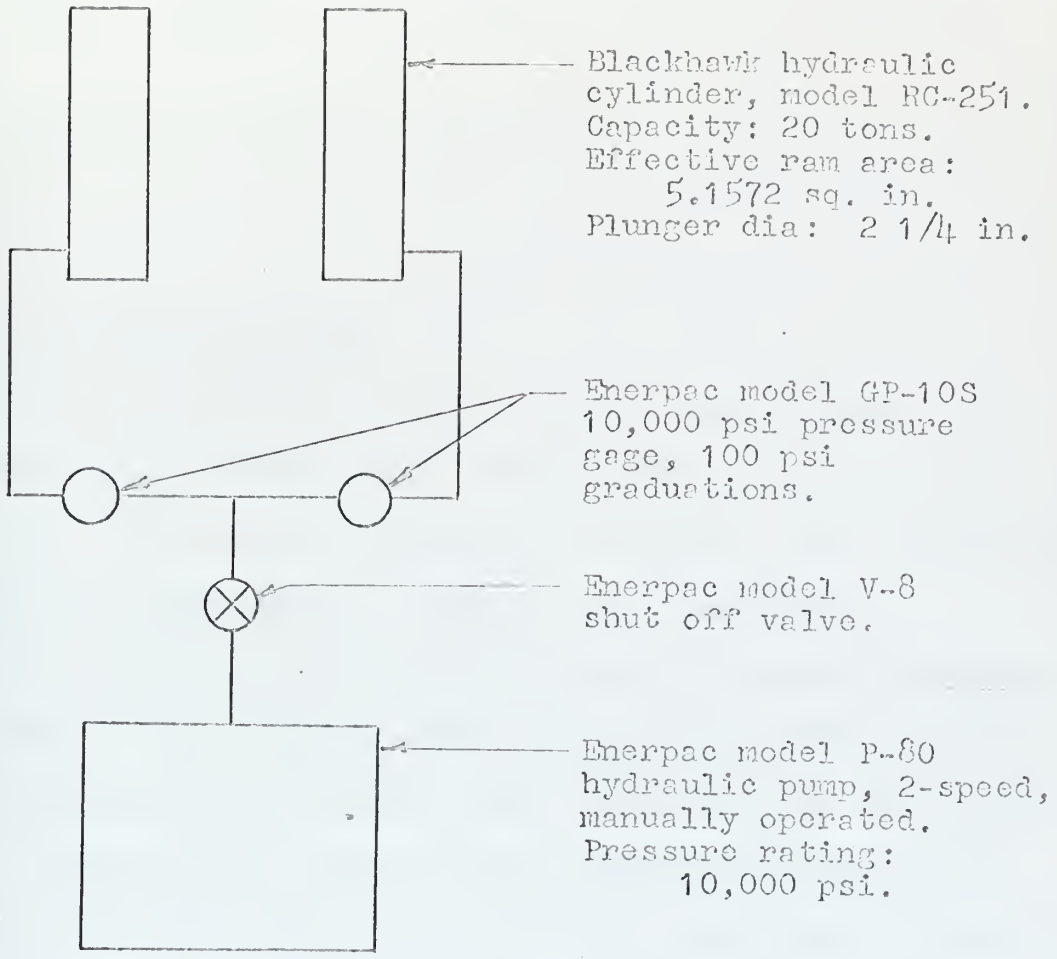

Figure A2. Schematic of hydraulic system.

to the plunger. Discussion of the effects will follow. The hydraulic pumps were fitted with additional stop valves for tighter holding of the load for extended periods of time.

Both test specimens were simply supported for all tests.

T-SECTION TEST SPECIMEN

The first specimen tested was the wide-flanged tee section shown in figure A3. Overall length of the sample was 28". The web was continuously welded to the flange with a fillet on both sides. Material was mild steel.

The simple supports for the tee section were fabricated from $\frac{1}{2}$" steel plate. The main support member was fitted with a slot and a knife edge to receive the web of the tee. During tests, the clearance between the web of the section and the sides of the slots was taken up with small wooden wedges. Those were primarily intended to steady and align the sample before the load was applied. It was felt that any effect on the simple support conditions would be negligible. In fact several wedges fell out from time to time after the load was applied.

For the axial compression tests, the cylinders bore directly against the web, centered at the neutral axis.

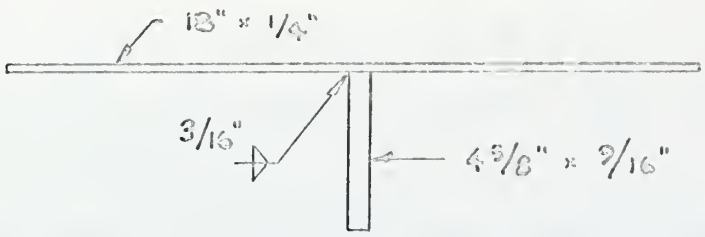

FIGURE A3. T-SECTION TEST SPECIMEN.

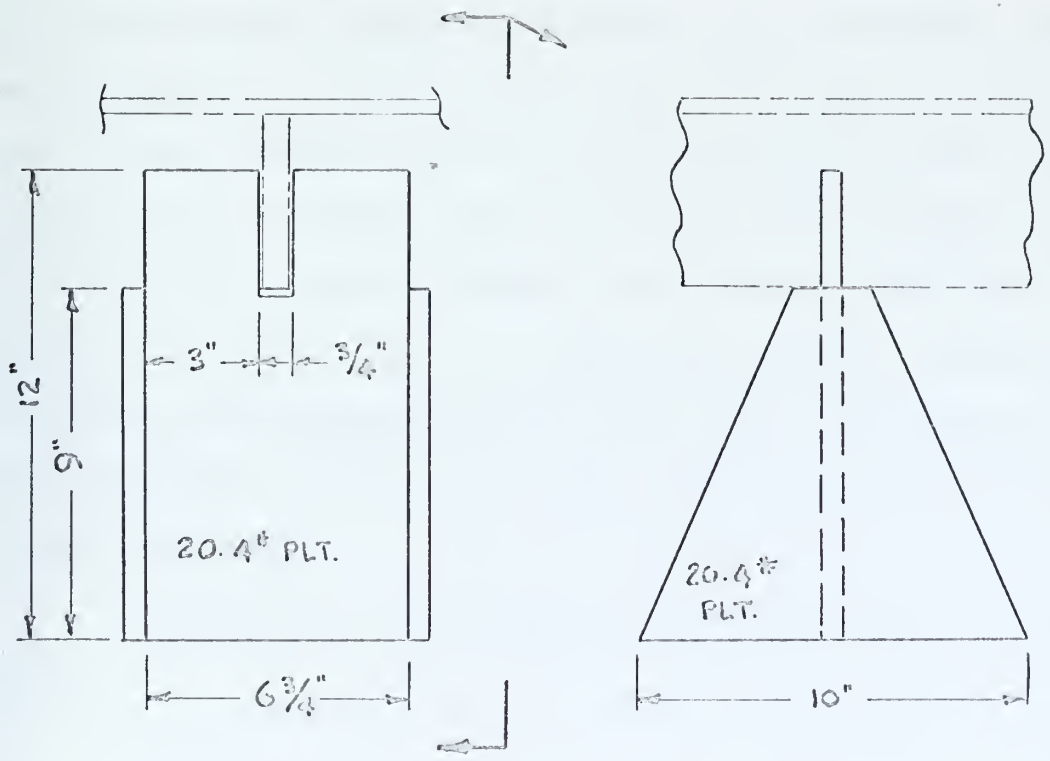

FIGURE A4. SIMPLE SUPPORT FOR T-SECTION.

The test section was instrumented across half the mid-span with one straight gage (BLH type FAE-25-12S6) at the web and five rectangular rosettes (BLH type FAER-25R-12S6). See figure B5.

The gages were connected in half bridge circuits, with one active and one dummy, through an Ellis 6-channel switch and balance unit and a Bean 10-channel switch and balance unit, to a Bean model 206B digital strain indicator. An idiosyncrasy in the Ellis unit forced the use of an individual dummy gage for each channel. One dummy was used for all 10 channels of the Bean unit.

The loads were applied with the hydraulic cylinders in the locations indicated schematically elsewhere. Care was taken not to exceed yield stress anywhere in the sample: The bottom of the web was the critical point. At least two sets of data were taken for each loading--one close to the maximum allowable, and one at about half that value. It was difficult to apply any specific predetermined load with the hydraulic system, but once a load was applied, its magnitude was known to close enough accuracy and it was able to be held.

A schematic of the hydraulic system is shown in figure A2 .

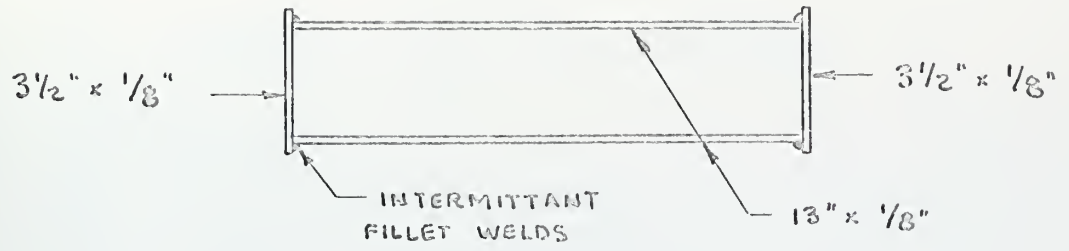

FIGURE A5. BOX GIRDER TEST SPECIMEN.

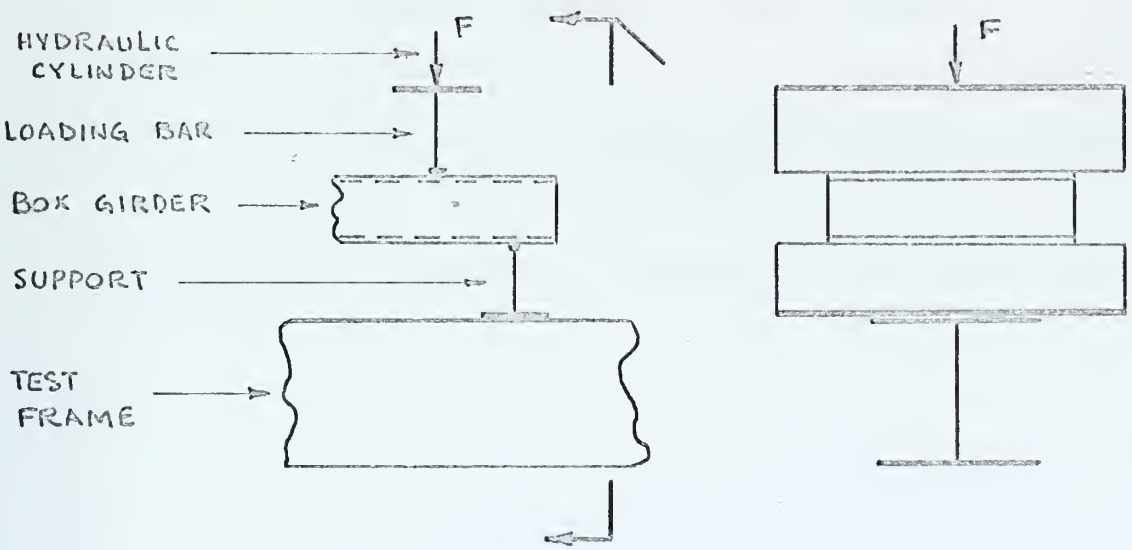

FIGURE A6. SCHEMATIC OF BENDING LOAD ON BOX GIRDER.

APPENDIX B

SUMMARY OF DATA AND CALCULATIONS

This appendix contains:

Curve of λ/b vs. L/B, T-section

Curve of λ/b vs. L/B, box girder

Sample moment of inertia and section modulus calculations

Curve of section modulus and section area vs. λ/b, T-section

Curve of section modulus and section area vs. λ/b, box girder

Sketch of strain gage location on T-section

Sketch of strain gage location on box girder

Summary of all test runs

Data used in calculating results, and principal stress calculations, for the following test runs: 3, 4, 6, 7, 8, 11, 13, 14, 15 and 16.

Calculation of internal and external moment balance, run 14

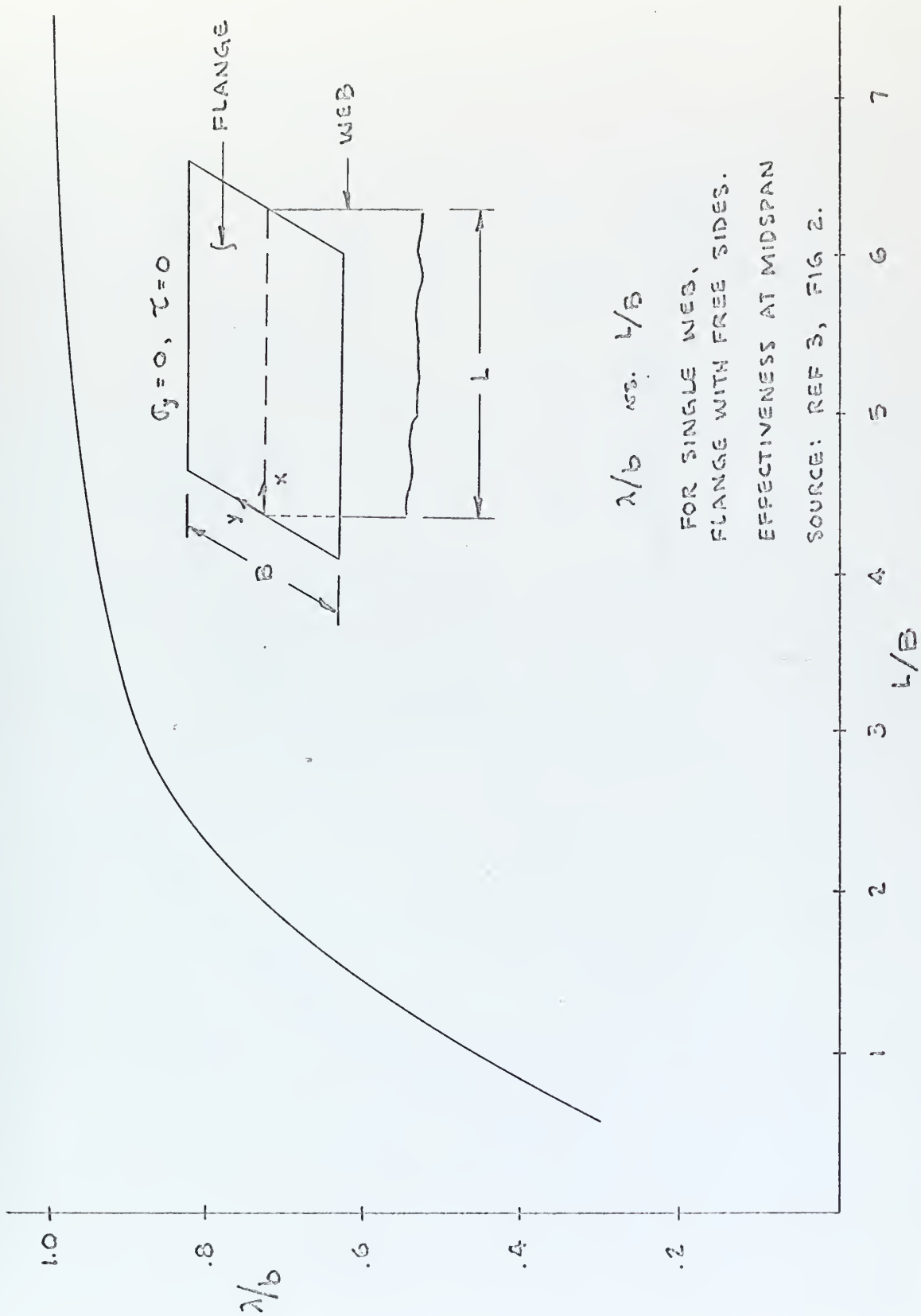
1.0
.8
.6
.4
.2
λ/b
1
2
3
4
5
6
7
L/B
λ/b vs. L/B
FOR SINGLE WEB,
FLANGE WITH FREE SIDES.
EFFECTIVENESS AT MIDSPAN
SOURCE: REF 3, FIG 2.
σy = 0, τ = 0
FLANGE
WEB
B
L
x
y

Figure B1.

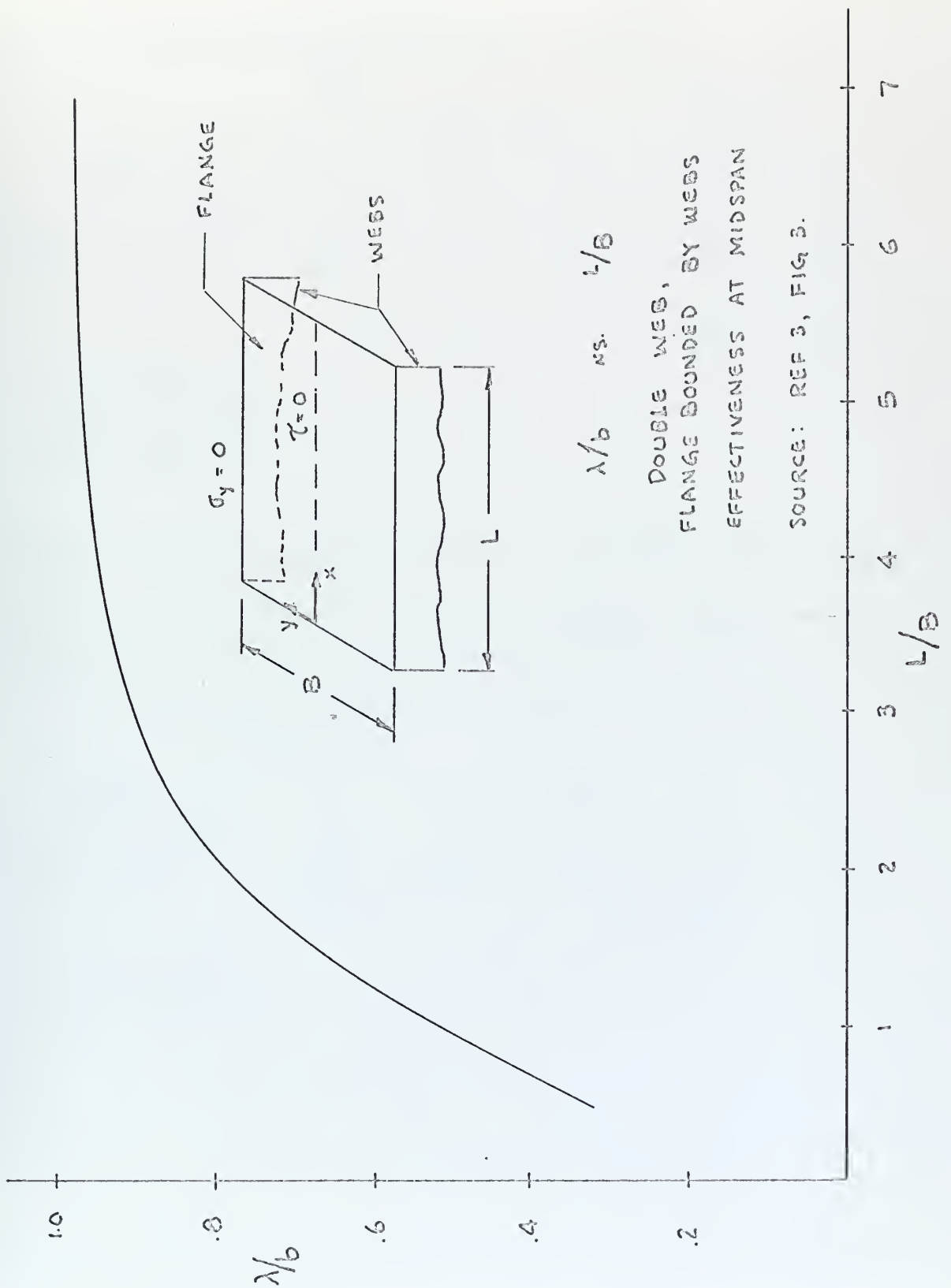
FLANGE
WEBS
$\sigma_y = 0$
$\tau = 0$
x
y
B
L
λ/b vs. L/B
DOUBLE WEB,
FLANGE BOUNDED BY WEBS
EFFECTIVENESS AT MIDSPAN
SOURCE: REF 3, FIG 3.
λ/b
1.0
.8
.6
.4
.2
1
2
3
4
5
6
7
L/B

Figure B2.

MOMENT OF INERTIA & SECTION MODULUS, T-SECTION, $\lambda/b = .75$

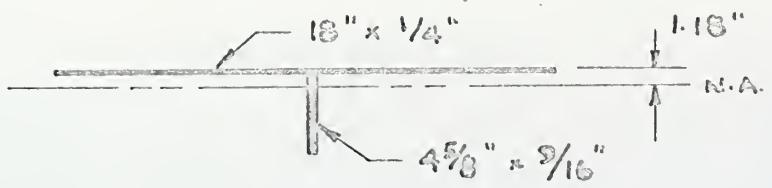

member	A	y	Ay	Ay^2	I_o
(18 x .75)" x 1/4"	3.38	.125	.42	.05	.02
4 5/8" x 9/16"	2.60	2.56	6.65	17.02	4.67
	5.98		7.07	Σ = 21.76	
	$\bar{y}$ = 1.18			$-Ay\bar{y}$ = 8.34	
				I = 13.42	

$I = 13.42 \text{ in}^4$

$Z_{fl} = 11.30 \text{ in}^3$

$Z_w = 3.60 \text{ in}^3$

MOMENT OF INERTIA & SECTION MODULUS, BOX GIRDER, $\lambda/b = 1.0$

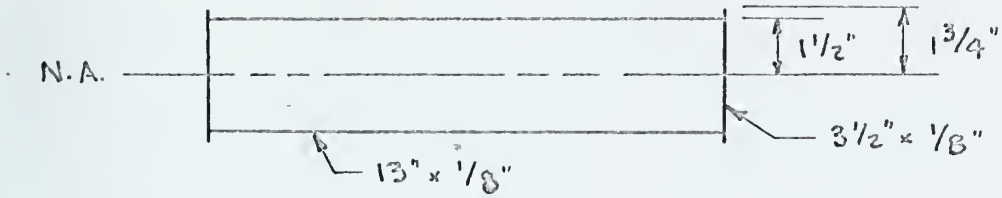

member	A	y	Ay^2	I_o
2 3 1/2" x 1/8"	.88	0	0	.90
2 13" x 1/8"	3.25	±1.44	6.75	--
	4.13		Σ = 7.65	

$I = 7.65 \text{ in}^4$

$Z_{fl} = 5.10 \text{ in}^3$

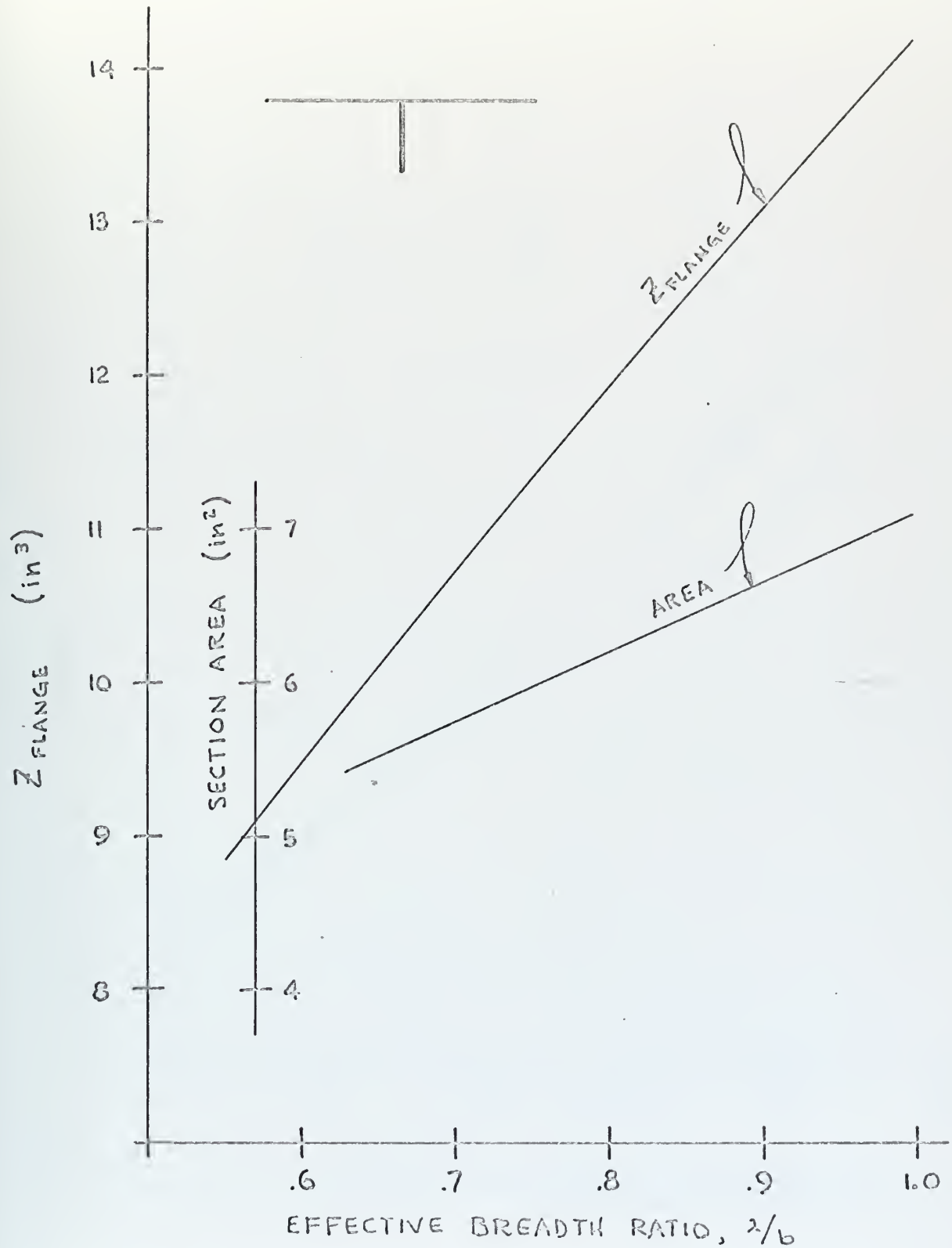

Figure B3. T-section characteristics.

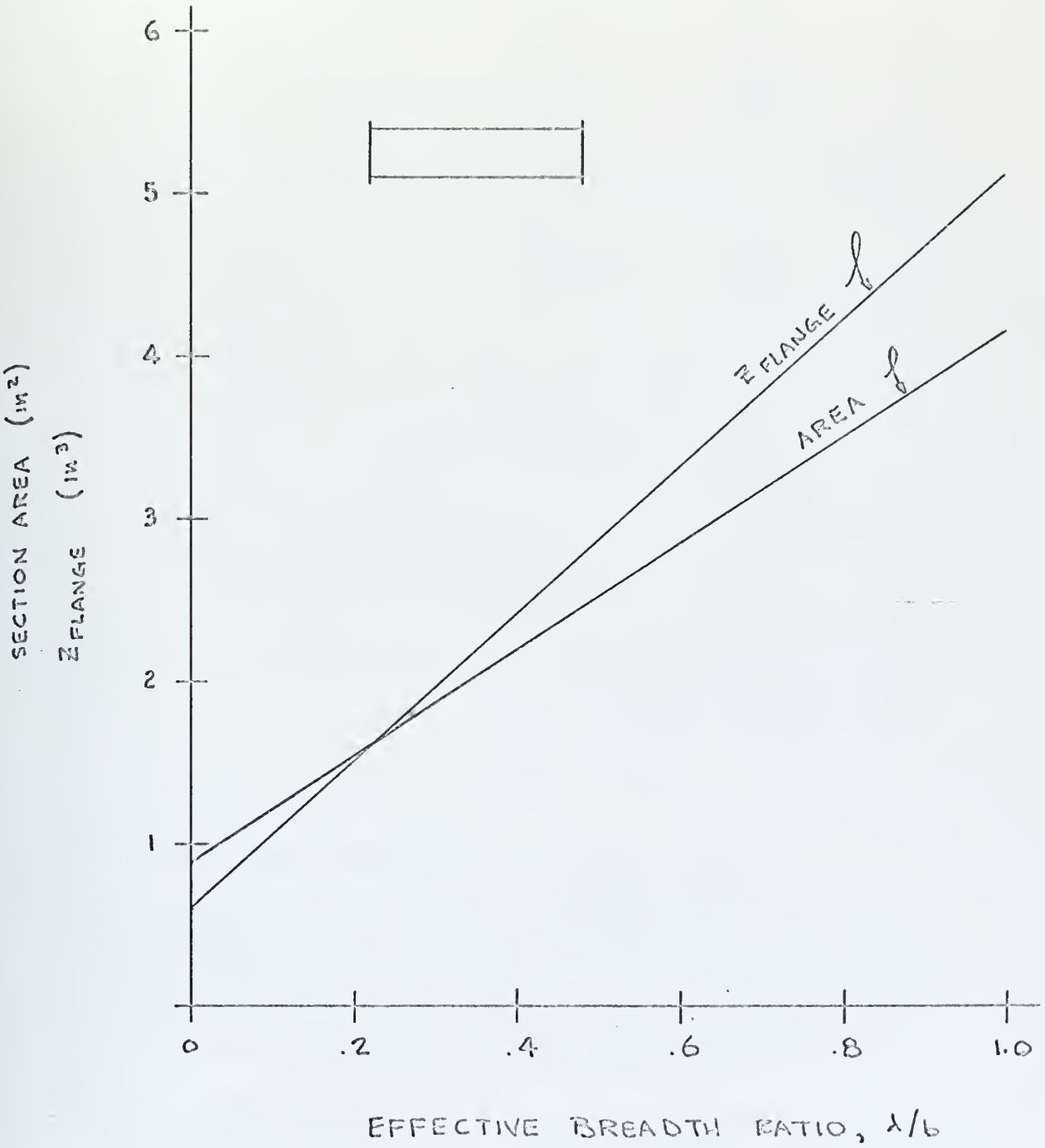

Figure B4. Box girder characteristics.

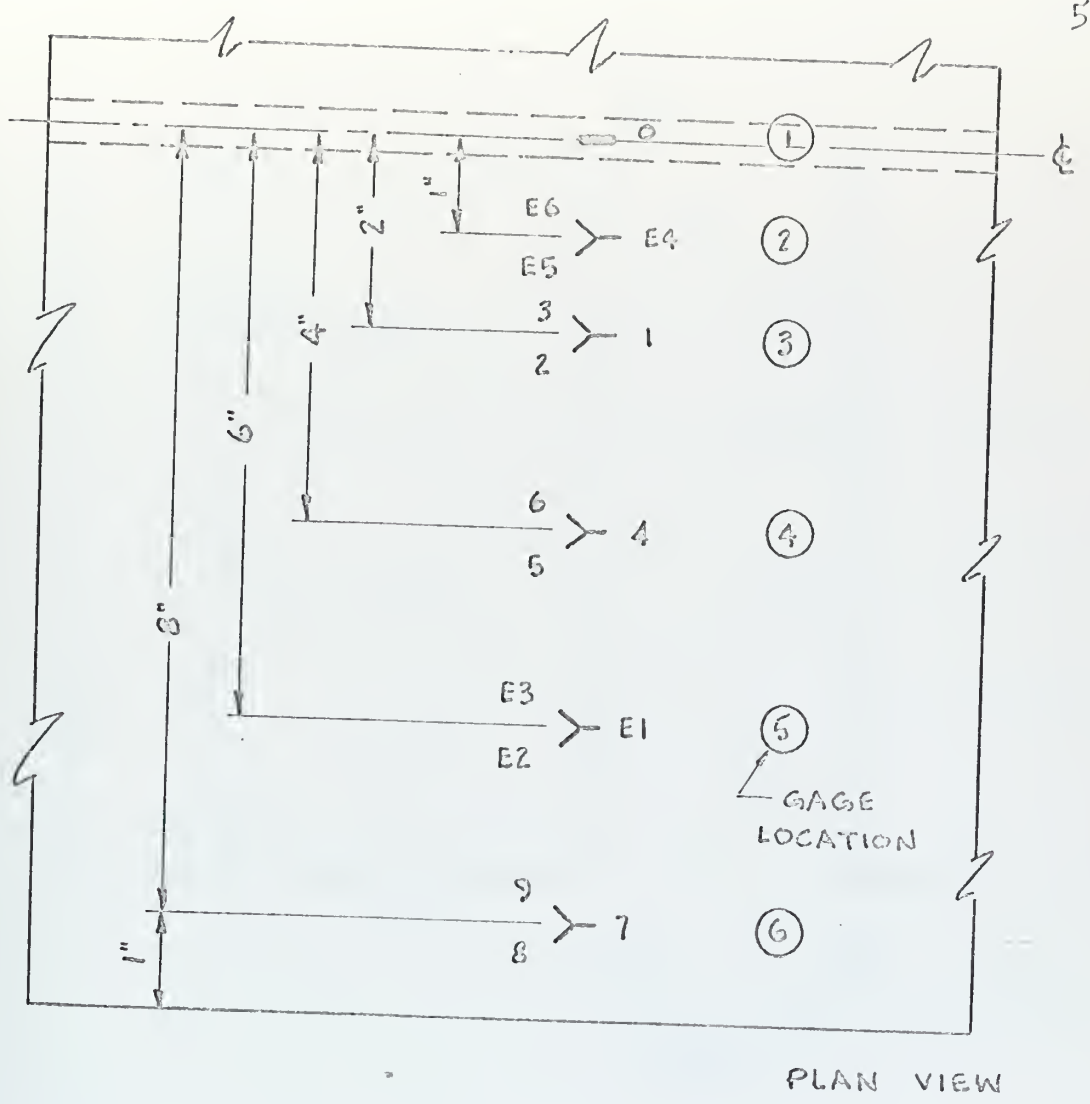

Gage 0. BLH type FAE-25-12S6L straight gage.

Gages 1 through E6. BLH type FAER-25R-12S6L rectangular rosettes. Due to a mix-up in identification of these gages, they were installed on the test specimen as though they were equiangular rosettes. The final results are uneffected, but calculations leading to principal stresses were more cumbersome.

"E" prefix denotes gages which were connected to the Ellis switch and balance unit. The remainder were connected to the Bean unit.

Figure B5. Gage location on T-section.

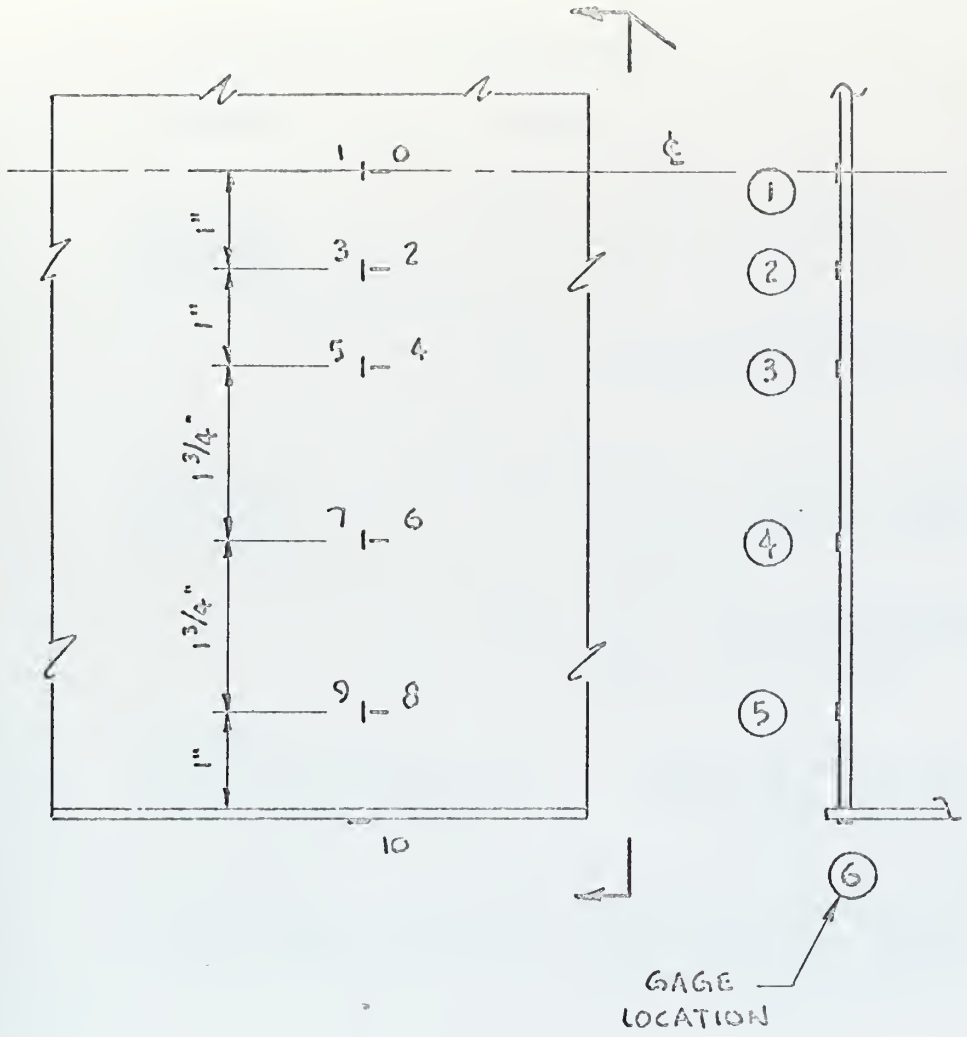

Gages 0 through 9. BLH type FAET-25T-12S9L 2-directional gages.

Gage 10. BLH type FAE-25-12S6L straight gage.

Figure B6. Gage location on box girder.

SUMMARY OF ALL TEST RUNS

Run no.	Loading	Remarks
1	2300 psi bending 4" lever arm	1) 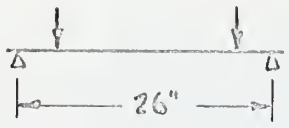 2) gage locations in figure apply to runs 1 through 7.
2	4450 psi bending 4" lever arm	1) gages 6 & 8 did not return to zero reading after load was removed; reading doubtful. 2) run 2 was made immediately after run 1 without returning to zero load.
3	4200 psi axial compression	1) 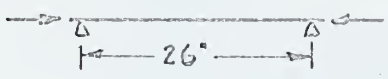
4	7025 psi axial compression	1) comment 2, run 2, applies. 2) dial indicator reading at mid-span was .0015".
5	4200 psi bending 4" lever arm	1) re-run of test run #2 to check the relative magnitudes of the shear stresses. 2) gages 6 & 8 appear to be functioning normally.
6	2300 psi bending 4" lever arm	1) load was applied through 3/4" diameter bearing rods rather than directly through the plunger head, (2 1/4" dia.)
7	4500 psi bending 4" lever arm	1) comment 2, run 2, applies.

Run no.	Loading	Remarks
8	Bending. 4" lever arm. Pressure = 1450 psi. M = 29,950 in-lb.	1) First load put on box girder. 2) Strain gages 0 through 9 in use through run # 12. 3) Loading on the webs through run # 14.
9	Bending. 4" lever arm. Pressure = 2800 psi. M = 57,900 in-lb.	1) Applied immediately after preceding load without returning to zero load. 2) Strain readings disproportionate to those in run 8.
10	Bending. 4" lever arm. Pressure = 1500 psi. M = 31,000 in-lb.	1) Comment 1, run 9, applies. 2) Large difference in strain readings from run 8, with approximately same moment. 3) Large change in zero readings after completion of runs 8, 9 and 10.
11	Bending. 7" lever arm. Pressure = 850 psi. M = 30,700 in-lb.	
12	Bending. 7" lever arm. Pressure = 1650 psi. M = 59,500 in-lb.	1) Comment 1, run 9, applies.
13	Bending. 4" lever arm. Pressure = 1525 psi. M = 31,400 in-lb.	1) Duplication of runs 8 and 10 with additional strain gage (gage # 10) in use. Gage # 2 disconnected.

Run no.	Loading	Remarks
14	Bending. 12½ lever arm. Pressure = 510 psi. M = 32,900 in-lb.	
15	Bending. 12½ lever arm. Pressure = 500 psi. M = 32,300 in-lb.	1) Loading directly on the flange in runs 15 and 16.
16	Bending. 4" lever arm. Pressure = 1325 psi. M = 27,400 in-lb.	

Data used in calculating results, run #3.

Loading: Axial compression.

Cylinder pressure: 4200 psi.

Applied force: 21,600 lbs.

STRAIN READINGS

Location	Gage no.	Average reading
1	0	-148
2	E4	-137
	E5	-50
	E6	-46
3	1	-129
	2	-44½
	3	-41
4	4	-99
	5	-34½
	6	defective
5	E1	-66½
	E2	-27½
	E3	-28
6	7	-49½
	8	defective
	9	-19½

PRINCIPAL STRESSES

Location	Stress
1	-4840 psi
2	-4090 psi
3	-3800 psi
4	-2970 psi
5	-2060 psi
6	-1485 psi

PRINCIPAL STRESS CALCULATIONS, RUN #3.

$$\sigma_1, \sigma_2 = E\left\{\frac{e_a + e_c}{2(1-\mu)} \pm \frac{1}{2(1+\mu)}\sqrt{(e_a - e_c)^2 + \left[2e_b - (e_a + e_c)\right]^2}\right\}$$

$$\tan 2\varphi = \frac{2e_b - (e_a + e_c)}{e_a - e_c}$$

$\mu = 0.285$

$E = 30 \times 10^6$ psi

	LOCATION	1	2	3	4	5	6
1	e_a		-46	-41		-28	
2	e_b	-148	-137	-129	-99	-66.5	-49.5
3	e_c		-50	-44.5		-27.5	
4	$e_a + e_c$		-96	-85.5		-55.5	
5	(4)/1.43		-67	-59.7		-38.8	
6	$e_a - e_c$		+4	+3.5		-.5	
7	$(6)^2$		16	12.2		.3	
8	$2e_b$		-274	-258		-133	
9	(8) - (4)		-178	-172.5		-77.5	
10	$(9)^2$		57600	51500		6000	
11	(7) + (10)		~ SAME AS (10)				
12	$\sqrt{(11)}$		178	172.5		77.5	
13	(12)/2.57		69.2	67		30.2	
14	(5) - (13)		-136.2	-126.7	-99 †	-68.6	-49.5 †
15	$\sigma_1 = E \times (14)$	-4840 *	-4090	-3800	-2970 †	-2060	-1485 †
16	(5) + (13)		+2.2	+7.3		-8.6	
17	$\sigma_2 = E \times (16)$		+66	+220		+258	
18	(9)/(6)		-44.5	-49.5		+155.	
19	2φ		88.7°	88.8°		89.6°	
20	φ		44.4°	44.4°		44.8°	
21	φ FROM ξ		0.6°	0.6°		0.2°	

* $e_b \times \frac{E}{1-\mu^2}$

† (2) × AVERAGE (14)/(2) FROM COLUMNS 2, 3 & 5.

Data used in calculation results, run #4.

Loading: Axial compression.

Cylinder pressure: 7025 psi.

Applied force: 36,220 lbs.

STRAIN READINGS

Location	Gage no.	Average reading
1	0	-252½
2	E4	-234
	E5	-82
	E6	-69
3	1	-214½
	2	-75
	3	-63½
4	4	-165½
	5	-55½
	6	defective
5	E1	-104½
	E2	-41
	E3	-35
6	7	-75½
	8	defective
	9	-25½

PRINCIPAL STRESSES

Location	Stress
1	-8250 psi
2	-6860 psi
3	-6300 psi
4	-4860 psi
5	-3140 psi
6	-2220 psi

PRINCIPAL STRESS CALCULATIONS, RUN #4.

$$\sigma_1, \sigma_2 = E\left\{\frac{\varepsilon_a + \varepsilon_c}{2(1-\mu)} \pm \frac{1}{2(1+\mu)}\sqrt{(\varepsilon_a - \varepsilon_c)^2 + \left[2\varepsilon_b - (\varepsilon_a + \varepsilon_c)\right]^2}\right\}$$

$$\tan 2\varphi = \frac{2\varepsilon_b - (\varepsilon_a + \varepsilon_c)}{\varepsilon_a - \varepsilon_c}$$

$\mu = 0.285$

$E = 30 \times 10^6$ psi

	LOCATION	1	2	3	4	5	6
1	ε_a		-69	-63.5		-35	
2	ε_b	-252.5	-234	-214.5	-165.5	-104.5	-75.5
3	ε_c		-82	-75		-41	
4	$\varepsilon_a + \varepsilon_c$		-151	-138.5		-76	
5	(4)/1.43		-105.1	-97		-53.1	
6	$\varepsilon_a - \varepsilon_c$		+13	+12.5		+6	
7	$(6)^2$		169	156		36	
8	$2\varepsilon_b$		-468	-429		-209	
9	(8) - (4)		-317	-290.5		-133	
10	$(9)^2$		100 000	84500		17800	
11	(7) ÷ (10)		≈ SAME AS (10)				
12	$\sqrt{(11)}$		317	290.5		133	
13	(12)/2.57		123.5	113.0		51.7	
14	(5) - (13)		-229.0	-210.0	-162 †	-104.8	-74 †
15	$\sigma_1 = E \times$ (14)	-8250 *	-6860	-6300	-4860	-3140	-2220
16	(5) + (13)		+18	+17		-1.4	
17	$\sigma_2 = E \times$ (16)		+540	+510		-42	
18	(9)/(6)		-24.2	-23.2		-22.2	
19	2φ		87.6°	87.5°		87.4°	
20	φ		43.8°	43.8°		43.7°	
21	φ FROM ε		1.2°	1.2°		1.3°	

* $\varepsilon_b \times E/(1-\mu^2)$

† (2) × AVERAGE (14)/(2) FROM COLUMNS 2, 3 & 5.

Data used in calculating results, run # 6.

Loading: Bending.

Cylinder pressure: 2300 psi.

Applied force: 11,850 lbs.

Lever arm: 4".

Applied moment: -47,400 in-lb.

STRAIN READINGS

Location	Gage no.	Average reading
1	0	-144
2	E4	-136½
	E5	-30
	E6	-40½
3	1	-124
	2	-26
	3	-35
4	4	-96½
	5	-18
	6	-31
5	E1	-72
	E2	-10
	E3	-25½
6	7	-52
	8	-13
	9	-29

PRINCIPAL STRESSES

Location	Stress
1	-4700 psi
2	-3830 psi
3	-3460 psi
4	-2720 psi
5	-2020 psi
6	-1630 psi

PRINCIPAL STRESS CALCULATIONS, RUN #6.

SEE RUNS 3 AND 4 FOR FORMULAE.

	LOCATION	1	2	3	4	5	6
1	ε_a		-40.5	-35	-31	-25.5	-29
2	ε_b	-144	-136.5	-124	-96.5	-72	-52
3	ε_c		-30	-26	-18	-10	-13
4	$\varepsilon_a + \varepsilon_c$		-70.5	-61	-49	-35.5	-42
5	(4)/1.43		-49.3	-42.6	-34.4	-24.8	-29.4
6	$\varepsilon_a - \varepsilon_c$		-10.5	-11	-13	-15.5	-16
7	$(6)^2$		110	121	169	241	256
8	$2\varepsilon_b$		-273	-248	-193	-144	-104
9	(8)-(4)		-202.5	-187	-144	-108.5	-62
10	$(9)^2$		41000	35000	20800	11800	3850
11	(7)+(10)		41110	35121	20969	12041	4106
12	$\sqrt{(11)}$		202.5	187	144.2	109	64.2
13	(12)/2.57		78.6	72.6	56.1	42.4	25.0
14	(5)-(13)		-127.9	-115.2	-90.5	-67.2	-54.4
15	$\sigma_1 = E \times (14)$	-4700*	-3830	-3460	-2720	-2020	-1630
16	(5)+(13)		+29.3	+30.0	+21.7	+17.6	+4.4
17	$\sigma_2 = E \times (16)$		+800	+900	+650	+528	+132
18	(9)/(6)		+19.3	+17.	+11.1	+6.96	+3.88
19	2φ		+87.1°	+86.6°	+84.8°	+81.8°	+75.2°
20	φ		+43.6°	+43.3°	+42.4°	+40.9°	+37.6°
21	φ FROM ξ		1.4°	1.7°	2.6°	4.1°	7.4°

* $\varepsilon_b \times E/(1-\mu^2)$

Data used in calculating results, run # 7.

Loading: Bending.

Cylinder pressure: 4500 psi.

Applied force: 23,150 lb.

Lever arm: 4".

Applied moment: -92,600 in-lb.

STRAIN READINGS

Location	Gage no.	Average reading
1	0	-288
2	E4	-273
	E5	-56
	E6	-71
3	1	-247
	2	-46½
	3	-62½
4	4	-192½
	5	-39
	6	-56
5	E1	-142½
	E2	-27½
	E3	-61
6	7	-106
	8	-26
	9	-52½

PRINCIPAL STRESSES

Location	Stress
1	-9410 psi
2	-7550 psi
3	-6800 psi
4	-5380 psi
5	-4180 psi
6	-3240 psi

PRINCIPAL STRESS CALCULATIONS, RUN #7.

SEE RUNS 3 AND 4 FOR FORMULAE.

	LOCATION	1	2	3	4	5	6
1	ε_a		-71	-62.5	-56	-61	-52.5
2	ε_b	-288	-273	-247	-192.5	-142.5	-106
3	ε_c		-56	-46.5	-39	-27.5	-26
4	$\varepsilon_a + \varepsilon_c$		-127	-109.0	-95	-88.5	-78.5
5	(4)/1.43		-88.9	-76.2	-66.5	-62	-55.0
6	$\varepsilon_a - \varepsilon_c$		-15	-16	-17	-33.5	-26.5
7	$(6)^2$		225	256	289	1120	702
8	$2\varepsilon_b$		-546	-494	-385	-285	-212
9	(8) - (4)		-419	-385	-290	-196.5	-133.5
10	$(9)^2$		176 000	148000	84000	38 700	17 900
11	(7) + (10)		176225	148256	84289	39 820	18 602
12	$\sqrt{(11)}$		419	385	290.3	199	136.2
13	(12)/2.57		163	150	113	77.5	53
14	(5) - (13)		-251.9	-226.2	-179.5	-139.5	-108
15	$\sigma_1 = E \times (14)$	-9410*	-7750	-6800	-5380	-4180	-3240
16	(5) + (13)		+74.1	+73.8	+46.5	+15.5	-2.0
17	$\sigma_2 = E \times (16)$		+2220	+2215	+1395	+465	-60
18	(9)/(6)		+27.9	+24.0	+17.1	+5.87	+5.04
19	2φ		87.8°	87.6°	86.7°	83.2°	78.8°
20	φ		43.9°	43.8°	43.4°	41.6°	39.4°
21	φ FROM ℓ		1.1°	1.2°	1.6°	3.4°	5.6°

* $\varepsilon_b \times E/(1-\mu^2)$

Data used in calculating results, run 8.

Loading: Bending.

Cylinder pressure: 1450 psi.

Applied force: 7480 lb (on webs).

Lever arm: 4"

Applied moment: 29,950 in-lb.

STRAIN READINGS

Location	Gage no.	Average reading
1	0	+30
	1	+114½
2	2	+17
	3	+83½
3	4	-14
	5	+47
4	6	-92
	7	-26½
5	8	-166½
	9	-124½

PRINCIPAL STRESSES

Location	Stress
1	+1970 psi
2	+1290 psi
3	0
4	-3040 psi
5	-6220 psi

Data used in calculating results, run 11.

Loading: Bending.

Cylinder pressure: 850 psi.

Applied force: 4380 lb (on web).

Lever arm: 7"

Applied moment: 30,700 in-lb.

STRAIN READINGS

Location	Gage no.	Average reading
1	0	+146½
	1	+174
2	2	+127
	3	+148
3	4	+76½
	5	+115
4	6	-67
	7	+28
5	8	-226½
	9	-100

PRINCIPAL STRESSES

Location	Stress
1	+6060 psi
2	+5240 psi
3	+3390 psi
4	-1775 psi
5	-7820 psi

Data used in calculating results, run 13.

Loading: Bending.

Cylinder pressure: 1525 psi.

Applied force: 7860 lb (on webs).

Lever arm: 4"

Applied moment: 31,400 in-lb.

STRAIN READINGS

Location	Gage no.	Average reading
1	0	+134½
	1	+175½
2	2	disconnected
	3	disconnected
3	4	+76
	5	+91
4	6	-47½
	7	-12
5	8	-188½
	9	-168
6	10	-188

PRINCIPAL STRESSES

Location	Stress
1	+5690 psi
2	--
3	+3150 psi
4	-1560 psi
5	-7280 psi
6	-5200 psi

PRINCIPAL STRESS CALCULATIONS, RUN 8.

$$\sigma_1 = \frac{E}{(1-\mu^2)} \left[e_1 + \mu e_2 \right]$$

$E = 27.6 \times 10^6$ psi

$\mu = .305$

	LOCATION	1	2	3	4	5
1	e_1	+30	+17	-14	-92	-166.5
2	e_2	+114.5	+83½	+47	-26.5	-124.5
3	μe_2	+34.9	+25.5	+14.3	-8.1	-38.0
4	$e_1 + \mu e_2$	+64.9	+42.5	0	-100.1	-204.5
5	σ_1	+1970	+1290	0	-3040	-6220

RUN 11.

	LOCATION	1	2	3	4	5
1	e_1	+146.5	+127	+76.5	-67	-226.5
2	e_2	+174	+148	+115	+28	-100
3	μe_2	+53	+45.1	+35.1	+8.6	-30.5
4	$e_1 + \mu e_2$	+199.5	+172.1	+111.6	-58.4	-257.0
5	σ_1	+6060	+5420	+3390	-1775	-7820

RUN 13

	LOCATION	1	2	3	4	5	6
1	e_1	+134.5		+76	-47.5	-188.5	-188
2	e_2	+175.5		+91	-12	-168	
3	μe_2	+52.5		+27.8	-3.7	-51.3	
4	$e_1 + \mu e_2$	+187.0		+103.8	-51.2	-239.8	
5	σ_1	+5690		+3150	-1560	-7280	-5200

Data used in calculating results, run 14.

Loading: Bending.

Cylinder pressure: 510 psi.

Applied force: 2630 lb (on webs).

Lever arm: $12\frac{1}{2}$"

Applied moment: 32,900 in-lb.

STRAIN READINGS

Location	Gage no.	Average reading
1	0	$+138\frac{1}{2}$
	1	+138
2	2	disconnected
	3	disconnected
3	4	+73
	5	$+97\frac{1}{2}$
4	6	$-61\frac{1}{2}$
	7	+43
5	8	$-233\frac{1}{2}$
	9	-45
6	10	-306

PRINCIPAL STRESSES

Location	Stress
1	+5490 psi
2	--
3	+3120 psi
4	-1470 psi
5	-7520 psi
6	-8450 psi

Data used in calculating results, run 15.

Loading: Bending.

Cylinder pressure: 500 psi.

Applied force: 2580 lb (on flange).

Lever arm: $12\frac{1}{2}$"

Applied moment: 32,200 in-lb.

STRAIN READINGS

Location	Gage no.	Average reading
1	0	$-251\frac{1}{2}$
	1	$-546\frac{1}{2}$
2	2	disconnected
	3	disconnected
3	4	$-218\frac{1}{2}$
	5	-532
4	6	-140
	7	$-388\frac{1}{2}$
5	8	-148
	9	$+103\frac{1}{2}$
6	10	$-397\frac{1}{2}$

PRINCIPAL STRESSES

Location	Stress
1	-12,850 psi
2	--
3	-11,300 psi
4	-7860 psi
5	-3540 psi
6	-10,950 psi

Data used in calculating results, run 16.

Loading: Bending.

Cylinder pressure: 1325 psi.

Applied force: 6840 lb (on flange).

Lever arm: 4"

Applied moment: 27,300 in-lb.

STRAIN READINGS

Location	Gage no.	Average reading
1	0	+382½
	1	+277
2	2	disconnected
	3	disconnected
3	4	+278½
	5	+204
4	6	+78
	7	+80
5	8	-149
	9	-166½
6	10	-168½

PRINCIPAL STRESSES

Location	Stress
1	+14,200 psi
2	--
3	+11,350 psi
4	+3120 psi
5	-6070 psi
6	-4650 psi

PRINCIPAL STRESS CALCULATIONS

$$\sigma_1 = \frac{E}{(1-\mu^2)} \left[e_1 + \mu e_2 \right]$$

$E = 27.6 \times 10^6$ psi

$\mu = .305$

RUN 14

	LOCATION	1	2	3	4	5	6
1	e_1	+138.5		+73	-61.5	-233.5	-306
2	e_2	+138		+97.5	+43	-45	
3	μe_2	+42		+29.8	+13.1	-13.7	
4	$e_1 + \mu e_2$	+180.5		+102.8	-48.4	-247.2	
5	σ_1	+5490		+3120	-1470	-7520	-8450

RUN 15

	LOCATION	1	2	3	4	5	6
1	e_1	-251.5		-218.5	-140	-148	-397.5
2	e_2	-546.5		-532	-388.5	+103.5	
3	μe_2	-172		-162	-118.5	+31.6	
4	$e_1 + \mu e_2$	-423.5		-370.5	-258.5	-116.4	
5	σ_1	-12850		-11300	-7860	-3540	-10 950

RUN 16

	LOCATION	1	2	3	4	5	6
1	e_1	+382.5		+278.5	+78	-149	-168.5
2	e_2	+277		+204	+80	-166.5	
3	μe_2	+84.5		+62.2	+24.4	-50.8	
4	$e_1 + \mu e_2$	+467		+340.7	+102.4	-199.8	
5	σ_1	+14200		+11350	+3120	-6070	-4650

MOMENT BALANCE - RUN 14.

INTERNAL MOMENT

FLANGES: $\lambda/b = .094$

$$\text{LOAD} = 8450(.094)(13)(.125) = 1290^{\#}$$

WEBS:

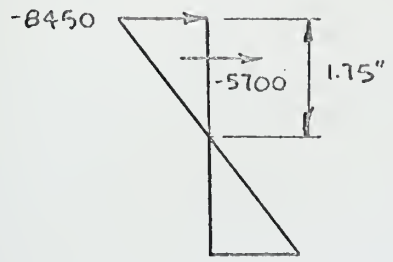

RESULTANT STRESS

$$= \frac{8450(1.75)}{2} = 7400^{\#}/in^2$$

RESULTANT FORCE

$$= 7400(.44)(1.75) = 5700^{\#}$$

MOMENT:

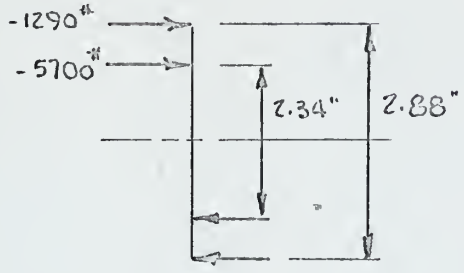

$$M = 1290(2.88) + 5700(2.34)$$

$$= 17,020 \text{ in-lb}$$

EXTERNAL MOMENT = 32,900 in-lb

APPENDIX C

ORIGINAL DATA

GAGE	0	E4	E5	E6	1	2	3	4	5	6	E1	E2	E3	7	8	9
ZERO	+3	+8	-2	0	0	0	0	0	-2	0	+6	+3	+3	+2	-5	-2
	0	+10	-2	0	0	0	0	-2	-2	-4	+8	+1	+7	0	-5	0
AVERAGE	+1½	+9	-2	0	0	0	0	-1	-2	-2	+7	+2	+5	+1	-5	-1
RUN 1	-135	-112	-62	+6	-115	-57	+5	-90	-58	+17	-65	-44	+15	-52	-247	+3
2300 psi	-137	-114	-64	+5	-115	-60	+3	-90	-58	+15	-75	-55	+5	-53	-243	+5
		-110	-62	+5							-65	-53	+5			
		-105	-62	+3							-63	-47	+7			
AVG.	-136	-110	-62½	+5	-115	-58½	+4	-90	-58		-65	-50	+8	-52½		+4
DIFF.	-137½	-119	-60½	+5	-115	-58½	+4	-89	-56		-72	-52	+3	-53½		+5
RUN 2	-269	-233	-87	-18	-227	-77	-10	-177	-73	-35	-130	-70	-25	-95	-277	-9
4450 psi	-273	-235	-90	-20	-232	-83	-15	-180	-75	-45	-133	-57	-8	-100	-287	-12
AVG.	-271	-234	-88½	-19	-229½	-80	-12½	-178½	-74		-131½	-63½	-16½	-97½		-10½
DIFF.	-272½	-243	-86½	-19	-229½	-80	-12½	-177½	-72		-138½	-65½	-21½	-98½		-9½
ZERO CHECK	+7	+18	-4	-5	+5	+5	+4	+5	+3	-50	+3	+2	-5	+8	-217	+8
	0	+23	-2	-2	0	-2	0	0	0	-55	+3	+5	0	+8	-225	+8

RUNS 1 & 2 — DATA

GAGE	0	E4	E5	E6	1	2	3	4	5	6	E1	E2	E3	7	8	9
ZERO	+2	+5	-3	0	-5	-2	-5	-3	-8	-99	+4	-5	0	+3	-334	+1
	-3	+2	-3	0	-7	-5	-7	-5	-8		+4	-5	-2	-1		-2
AVG.	-½	+3½	-3	0	-6	-3½	-6	-4	-8		+4	-5	-1	+1		-½
RUN 3	-150	-132	-53	-45	-135	-48	-47	-102	-45	DEFLECTED	-62	-40	-40	-50	DEFLECTING	-20
4200 psi	-147	-135	-53	-47	-135	-48	-47	-104	-40		-63	-25	-18	-47		-20
AVG.	-148½	-133½	-53	-46	-135	-48	-47	-103	-42½		-62½	-32½	-29	-48½		-20
DIFF.	-148	-137	-50	-46	-129	-44½	-41	-99	-34½	WIRE	-66½	-27½	-28	-49½	WIRE	-19½
RUN 4	-255	-232	-85	-69	-222	-80	-72	-170	-67	ARM	-97	-47	-45	-77	ARM	-27
7025 psi	-251	-229	-85	-69	-219	-77	-67	-169	-60		-104	-45	-27	-72		-26
AVG.	-253	-230½	-85	-69	-220½	-78½	-69½	-169½	-63½		-100½	-46	-36	-74½		-26
DIFF.	-252½	-234	-82	-69	-214½	-75	-63½	-165½	-55½		-104½	-41	-35	-75½		-25½
ZERO CHECK †	-17	-15	-7	-7	-20	-8	-12	-15	-12		+5	-4	+1	+6		-5
	-5	-5	0	+3	-8	+3	-4	-5	-5		+5	+3	-5	+10		+3

† AFTER ½ HOUR TIME LAPSE.

RUNS 3 & 4 — DATA

GAGE	0	E4	E5	E6	1	2	3	4	5	6	E1	E2	E3	7	8	9
ZERO	-1	-4	+2	+3	-2	-2	0	-2	-5	-2	-5	+3	+8	-3	-2	-5
	-2	-2	+2	+3	-4	-3	-2	-2	-7	-5	-7	+5	0	-5	-4	-7
AVG.	-1½	-3	+2	+3	-3	-2½	-1	-2	-6	-3½	-6	+4	+4	-4	-3	-6
RUN 5 4200 psi	-272	-255	-25	-80	-235	-23	-75	-184	-25	-80	-130	-7	-82	-107	-12	-80
	-272	-255	-27	-79	-235	-23	-75	-185	-24	-80	-129	-5	-67	-107	-9	-77
AVG.	-272	-255	-26	-79½	-235	-23	-75	-184½	-24½	-80	-129½	-6	-74½	-107	-10½	-78½
DIFF.	-270½	-252	-28	-82½	-232	-20½	-74	-182½	-18½	-76½	-123½	-10	-78½	-103	-7½	-72½
ZERO CHECK	-2	-4	-2	+2	-2	-3	-1	-4	-14	-10	+2	-3	-5	-13	-11	-14

RUN 5 - DATA

GAGE	0	E4	E5	E6	1	2	3	4	5	6	E1	E2	E3	7	8	9
ZERO	-4	-4	-2	0	-5	-2	-2	-2	-4	-1	-7	-8	+3	-5	-2	-3
	-4	-4	+2	+3	-5	-2	-3	-2	-4	-1	-4	-2	-3	-3	-2	-3
AVG.	-4	-4	0	+1½	-5	-2	-2½	-2	-4	-1	-5½	-5	0	-4	-2	-3
RUN 6 2300 psi	-149	-142	-30	-39	-130	-28	-37	-99	-22	-32	-75	-15	-27	-57	-15	-32
	-147	-139	-30	-39	-128	-28	-38	-98	-22	-32	-80	-15	-24	-55	-15	-32
AVG.	-148	-140½	-30	-39	-129	-28	-37½	-98½	-22	-32	-77½	-15	-25½	-56	-15	-32
DIFF.	-144	-136½	-30	-40½	-124	-26	-35	-96½	-18	-31	-72	-10	-25½	-52	-13	-29
RUN 7 4500 psi	-295	-277	-55	-70	-252	-50	-65	-195	-44	-57	-149	-35	-70	-110	-29	-57
	-289	-277	-57	-69	-252	-47	-65	-194	-42	-57	-147	-30	-52	-110	-27	-54
AVG.	-292	-277	-56	-69½	-252	-48½	-65	-194½	-43	-57	-148	-32½	-61	-110	-28	-55½
DIFF.	-288	-273	-56	-71	-247	-46½	-62½	-192½	-39	-56	-142½	-27½	-61	-106	-26	-52½
ZERO CHECK	-15	-15	-2	-5	-15	-5	-10	-10	-10	-8	-10	-5	-4	-9	-10	-14

RUNS 6 & 7 - DATA

GAGE	0	1	2	3	4	5	6	7	8	9
ZERO	-2	-4	0	-2	0	+2	-2	+1	-2	0
	-2	-4	0	0	0	+2	-2	0	-2	-2
AVERAGE	-2	-4	0	-1	0	+2	-2	+½	-2	-1
RUN 8	+28	+111	+17	+83	-13	+50	-93	-25	-167	-124
1450 psi	+28	+110	+17	+82	-15	+48	-95	-27	-170	-127
AVG.	+28	+110½	+17	+82½	-14	+49	-94	-26	-168½	-125½
DIFF.	+30	+114½	+17	+83½	-14	+47	-92	-26½	-166½	-124½
RUN 9	+553	+361	+520	+307	+405	+263	+63	+130	-309	-195
2800 psi	+553	+361	+518	+307	+405	+263	+63	+128	-310	-195
RUN 10	+316	+251	+295	+205	+230	+158	+35	+50	-154	-132
1500 psi										
ZERO	+92	+22	+93	+18	+87	+20	+62	+30	+65	+48

RUNS 8, 9 & 10 - DATA

GAGE	0	1	2	3	4	5	6	7	8	9
ZERO	+1	0	0	0	0	-4	-5	-4	-4	-5
	-2	-2	-2	-2	-2	-4	-5	-5	-5	-5
AVG.	-½	-1	-1	-1	-1	-4	-5	-4½	-4½	-5
RUN 11	+147	+173	+127	+147	+76	+112	-72	+32	-230	-105
850 psi	+145	+173	+125	+147	+75	+110	-72	+33	-232	-105
AVG.	+146	+173	+126	+147	+75½	+111	-72	+32½	-231	-105
DIFF.	+146½	+174	+127	+148	+76½	+115	-67	+28	-226½	-100
RUN 12	+438	+293	+398	+265	+293	+238	-34	+143	-415	-133
1650 psi	+438	+295	+398	+265	+292	+238	-35	+143	-415	-134
ZERO	-2	-12	-3	-12	-4	-15	-10	-15	-12	-14

RUNS 11 & 12 - DATA

GAGE	0	1	2	3	4	5	6	7	8	9	10
ZERO	-4	-4	DISCONNECTED	-10	-2	-2	-4	-2	-3	-5	-4
	-5	-5		-12	-4	-4	-5	-4	-5	-5	-7
AVG.	-4½	-4½		-11	-3	-3	-4½	-3	-4	-5	-5½
RUN 13 1525 psi	+130	+171		+125	+73	+88	-52	-15	-193	-173	-193
	+130	+171		+125	+73	+88	-52	-15	-192	-173	-194
AVG.	+130	+171			+73	+88	-52	-15	-192½	-173	-193½
DIFF.	+134½	+175½			+76	+91	-47½	-12	-188½	-168	-188
ZERO	-14	-13		-22	-13	-13	-15	-12	-14	-12	-10

RUN 13 - DATA

GAGE	0	1	2	3	4	5	6	7	8	9	10
ZERO	0	-1		-8	-3	-2	-6	-2	-8	-3	-3
AVERAGE †	-7	-8		-17	-10	-10	-14	-10	-14	-10	-9
RUN 14	+135	+133		+105	+66	+90	-72	+36	-245	-52	-313
510 psi	+128	+127		+100	+60	+85	-79	+30	-250	-50	-317
AVG.	+131½	+130	DISCONNECTED		+63	+87½	-75½	+33	-247½	-55	-315
DIFF.	+138½	+138			+73	+97½	-61½	+43	-233½	-45	-306
ZERO	-14	-15		-25	-17	-18	-22	-18	-20	-17	-15
ZERO	-22	-62	RECONNECTED	-65	-24	-52	-17	-19	-19	+5	-15
AVERAGE †	-38½	-73			-36½	-72	-15½	-56½	-22	-32	-39½
RUN 15	-290	-619		-632	-255	-604	-154	-445	-170	+73	-437
500 psi	-290	-620		-634	-255	-604	-157	-445	-170	+70	-437
AVG.	-290	-619½			-255	-604	-155½	-445	-170	+71½	-437
DIFF.	-251½	-546½			-218½	-532	-140	-388½	-148	+103½	-397½
ZERO	-55	-84		-94	-48	-92	-14	-94	-25	-69	-64

† AVERAGE BEFORE & AFTER LOADING.

RUNS 14 & 15 - DATA

GAGE	0	1	2	3	4	5	6	7	8	9	10
ZERO	-55	-82	DEBONDED	-92	-47	-92	-15	-95	-25	-74	-63
AVERAGE †	+2½	-52		-64½	-½	-71	+10	-90	-25	-90½	-91½
RUN 16 1325 psi	+385	+225		+178	+278	+133	+88	-10	-174	-257	-260
DIFF.	+382½	+277			+278½	+204	+78	+80	-149	-166½	-168½
ZERO	+60	-22		-37	+46	-50	+35	-85	-25	-107	-120

† AVERAGE BEFORE AND AFTER LOADING.

RUN 16 - DATA

APPENDIX D

ACKNOWLEDGEMENTS

The author wishes to express his gratitude to Professor Alaa Mansour, M.I.T., for his support of this project, as well as his guidance, encouragement and patience throughout its duration, and to Professor William Murray, M.I.T., for his advise, particularly in the use of strain gages.

APPENDIX E

REFERENCES

1. Schade, H.A., "The Effective Breadth of Stiffened Plating Under Bending Loads," Transactions, SNAME, 1951.

2. Schade, H.A., "The Effective Breadth Concept in Ship-Structure Design," Transactions, SNAME, 1953.

3. Mansour, A.E.,"Effective Flange Breadth of Stiffened Plates Under Axial Tensile Load or Uniform Bending Moment," Journal of Ship Research, March, 1970.

4. Murray, W.M., "Rosette Analysis," part of a series of lectures presented at the Massachusetts Institute of Technology, July, 1969.

5. Timoshenko, S.P., Theory of Elastic Stability, 2nd Edition, McGraw-Hill, New York, 1961.

6. Mansour, A.E., "On the Non-linear Theory of Orthotropic Plates," to be published in the Journal of Ship Research.

7. Schade, H.A., "Thin-walled Box Girder -- Theory and Experiment," Report no. NA-64-6, Institute of Engineering Research, University of California, June, 1964.

Thesis
H1645 Hamma
118364
Experimental determination of effective breadth of wide flange sections.